POLITECNICO DI TORINO

Department of Mechanical and Aerospace Engineering (DIMEAS)

Master Degree in Biomedical Engineering

Preparation and characterization of bioartificial polymeric nanoparticles for microRNA release

Supervisor

Prof.ssa Valeria Chiono

Co-supervisor

Dott.ssa Clara Mattu

Candidate

Marcello Aramu

Academic Year 2018/2019

INDEX

Abstract

Currently, myocardial infarction (MI) is the cause of around 50% of the deceases among cardiovascular diseases (CVDs). The massive loss of cardiomyocytes (CMs) due to MI can lead to pathological remodeling of the left ventricle (LV), resulting in deterioration of heart structure and function. Moreover, the adult myocardium has a limited capacity for endogenous regeneration and repair because adult cardiomyocytes are terminally differentiated cells without replication ability after injury. To date, transplantation remains the only therapeutic option in the clinics for end-stage heart failure, while the stem cell-based regenerative medicine strategies moderately improve cardiomyocyte survival, but do not allow cardio-myogenesis. This has prompted the need for new regenerative medicine approaches. MicroRNAs (miRNAs), small noncoding RNAs, have been shown to have a key role in cardiac development. Moreover, a combination of four miRNAs (miR-Combo) has been reported to promote the direct conversion of mouse cardiac fibroblasts into cardiomyocytes, using viral vectors [1].

However, a safer administration of such reprogramming agents requires their encapsulation inside specific vehicles. In this contest, several viral and non-viral systems have been proposed for miRNA delivery. Despite viral vectors allow high transfection efficiency of the genetic material into the target cells, their application in the clinics is limited by some disadvantages, including high cost and the risk for off-target effects, immunogenicity and insertional mutagenesis when using integrating vectors. Non-viral systems could represent safer systems for miRNA release.

In this work, bioartificial polymeric nanoparticles based on Chitosan (CS) and poly(lactic-co-glycolic acid) (PLGA) were produced by nanoprecipitation technique for the entrapment and release of miRNAs. CS was chosen for the presence of positively charged amino groups able to electrostatically interact with the negative phosphate groups of the miRNA, forming complexes. PLGA was used to give stability and protection to CS/miRNA complexes, moreover it is biocompatible and biodegradable polymer approved by FDA (Food and Drug Administration).

An initial protocol for nanoparticle preparation was derived from literature [2] as described in Material and Methods section (“First Method). The

nanoparticles realized with this method shown a size of about 210 nm and PDI 0.18 as regard blank nanoparticles and 220 nm and PDI of 0.17 as regard miRNA-loaded nanoparticles. The percentage Yield was around 37% and 50% for blank nanoparticles and miRNA-loaded nanoparticles respectively. However, the problems seen with this method, including the presence of surfactant at the end of the process, toxicity of the solution and probably miRNA damage because homogenization phases, forced us to modify the protocol.

In order to avoid the formation of more nanoparticle population, the surfactant used was replaced with a PLGA-COOH which in any case guarantees the stability of suspended nanoparticles. The chitosan solution used was replaced with a higher pH solution (5.4), in order to solve the toxicity problem. Finally, the homogenization phase has been removed.

With the new method we studied the interaction between the positive ammine groups (N) of chitosan and the negative phosphate groups (P) of the miRNA in order to find an interaction strong for complexes formation but enough to allow a miRNA release. Has been investigated six different N/P ratios (0.7, 1.75, 3, 5, 8 and 15), obtained by varying the amount of chitosan and maintaining that of miRNA fixed. Subsequently the PLGA-COOH solution has been added.

This work of thesis focused on evaluation of nanoparticles in terms of Size and PDI, Zeta potential, miRNA Entrapment Efficiency, Release, Morphology and Stability (in water and in DMEM-FBS).

On the basis of these studies, considerations and choices have been made in order to choose the best condition, trying to optimize the process.

The sample that showed the most promising features at the end of this work was the nanoparticles with N/P ratio of 8.

In details, the nanoparticles realized in the last step show an average size ~200 nm, low PDI (<0.2) and positive zeta potential of about 28 mV. The entrapment efficiency exhibited excellent results (~90%) and the release was around 70% from 7th day to 14th day. The morphology study, made through SEM, confirmed the nanoparticle spherical shape and their nanometric dimensions. Finally, these nanoparticles were found to be stable for 7 day in water but only 1 in DMEM-FBS because of their interaction with the protein in culture medium.

In conclusion, the developed bioartificial polymeric nanoparticles, after further improvements, could be tested in the future as delivery system for reprogramming agents (miRNA) for cardiac reprogramming.

Chapter 1- General Introduction

1.1 Aim of the work

Nanocarrier-based drug delivery systems represent engineered technologies for the targeted delivery and/or controlled release of therapeutic agents into a specific target tissue. Drugs could improve human health and extend life expectancy, however, their delivery systems should be optimized to improve their efficacy and specificity based on the type of administration route, such as systemic (oral, enteral, parenteral) or local administration (topical).

In the past few decades, drug delivery systems have greatly evolved and are projected to further improve in the near future. Biomedical engineering and nanotechnology have significantly contributed to the evolution of these systems, improving their design to overcome physiological barriers and increasing the efficiency of drug release or enhancing the transport through the circulatory system and drug uptake by cells and tissues. Drug delivery systems may now be designed to control the rate at which a drug is released and its targeted release. Typically, drug delivery system reported in literature are based on liposomes, polymerosomes, polymeric micelles, microbubbles, nanoparticles and dendrimers. They can be used depending on the type of drug encapsulated and the area where the cargo should be released.

The objective of this thesis was the preparation and characterization of bioartificial polymers nanoparticles (PLGA and Chitosan) able to incapsulate and release reprogramming agent, based on microRNA (miRNA), for future application in the direct reprogramming of fibroblasts into cardiomyocytes. The thesis is part of the research activity within the ERC project BIORECAR (www.biorecar.polito.it), which aims at inducing the direct conversion of scar-forming fibroblasts into cardiomyocytes using miRNAs, as an advanced strategy for myocardial regeneration, as to ensure a better lifestyle for infarcted patients.

Recently, literature has reported that specific miRNAs (miR-1, miR-208, miR-499, and miR-133) are able to promote the direct reprogramming of mouse fibroblasts into cardiomyocytes [3]. However, in those studies, direct reprogramming in mouse model has been performed using viral vectors.

The incorporation of miRNAs within NPs could allow a safer approach for miRNA *in vivo* administration and thus represents one main objective in BIORECAR.

Several miRNA delivery systems have been proposed in the literature, mainly based on cationic polymers, liposomes and dendrimers. The objective of this thesis was that to develop NPs for miRNA release using commercially available polymers, including chitosan and PLGA. PLGA was chosen as a biomaterial due to its biocompatibility, biodegradability, shape stability *in vivo* and because it is widely used as a polymer able to protect the drugs from degradation. Chitosan, derived from chitin natural polymer, was selected for its biocompatibility and because it possesses amino groups, which – when protonated- are able to interact with the negative phosphate groups of miRNA, increasing miRNA entrapment efficiency. Hence the aim was that to obtain NPs with high encapsulation ability, and sufficient stability in physiological conditions, to allow future *in vivo* application. Considering that NPs were based on synthetic and natural polymers, they were defined "bioartificial".

In this thesis work, the nanoparticles were realized through a nanoprecipitation technique, starting from a protocol reported in the literature and modifying/optimizing such protocol when necessary. The chitosan-miRNA complexes, obtained by electrostatic interaction between the two components, were subsequently combined with PLGA to obtain chitosan-PLGA nanoparticles – miRNA loaded.

The aim was that to deeply improve the literature protocol by addressing its critical issues. In particular, the presence of Poloxamer, used as surfactant for nanoparticle stability in solution, was found at the end of the process causing a possible poloxamer micelles formation. Moreover, the pH nanoparticles solution is resulted too acid causing possible toxicity problems for *in vivo* application. Finally, because the homogenization phases there are possibility to damage the miRNA.

Consequently, the poloxamer was removed and interaction between chitosan and PLGA was enhanced by employing a PLGA with terminal COOH groups (PLGA-COOH). PLGA-COOH is more hydrophilic than PLGA and allows for electrostatic interactions with chitosan. Moreover, the homogenization phase has been removed and a milder process was introduced to avoid miRNA damages. Finally, a chitosan solution with higher pH (5.4) was employed to solve the cytocompatibility issues.

A preliminary study based on Size, PDI, Zeta Potential and Stability in water was done to analyze and optimize the CS-miRNA interaction by evaluating different ratios between the amino groups (N) in chitosan and the phosphate groups (P) in the oligonucleotides. The aim of this study was to determine an optimal N/P ratio which allows sufficiently strong interactions for the formation of CS/miRNA complexes without hindering miRNA release.

Further aims were to evaluate the bioartificial NPs in terms of Size and PDI as well as Surface zeta potential that is a fundamental parameter to characterize the interaction of NPs with the medium. The yield of NP formation was evaluated, giving information on the efficiency of NP preparation.

Moreover, an optimum delivery system must have a high encapsulation efficiency and a good release ability, in fact, they can positively influence *in vitro* cell transfection and *in vivo* therapeutic response. Therefore, these two parameters have been studied.

Nanoparticles must also maintain stability for an enough day, therefore stability tests were carried out in water and DMEM.

In order to verify the NPs spherical shape, has been done a morphology study by SEM.

Finally, the toxicity test was repeated to demonstrate the biocompatibility of nanoparticle solution.

In this thesis, detailed physicochemical characterization of nanoparticles was achieved from the training experience at the Bioengineering and Biolab laboratories of the Department of Mechanical and Aerospace Engineering (DIMEAS) at Politecnico di Torino.

1.2 Introduction

In the last decades, new approaches were developed for the treatment of damaged tissues/organs by pathologies such as myocardial infarct and tumors.
Despite many progresses has been made, today the treatment of these pathologies is still a challenge faced by biomedical researchers and companies. In this context, highly specialized and less invasive devices are needed, exploiting the nanomedicine field.
As regard, the treatment of myocardium infarcted, the principal problems are the massive cardiomyocyte death and the formation of fibrotic and not contractile scars populated by cardiac fibroblasts[4]. The traditional strategies are based on tissue engineering and cellular therapy. In addition to these methods, a new regenerative medicine approach was investigated recently to directly convert fibroblasts into cardiomyocytes. This transdifferentiation has been demonstrated by Ieda et al. in 2010[5], which they have discovered a combination of transcriptional factors that, if stimulated, will induce the direct conversion of the murine fibroblasts into cardiomyocytes by genetic therapy (viral vectors). Thenceforth, several reprogramming agents, such as microRNAs, are used in numerous experiments. The microRNA combination, or "miR-Combo", permits to reduce the risks linked to using of viral vectors. However, these oligonucleotides must be encapsulated into delivery systems in order to promote the local release, control the kinetic and avoid undesirable effects[6].
Polymeric-based nanoparticles are drug delivery systems widely studied in literature for their advantages compared to other nanocarrier systems such as liposomes, polymeric micelles, microbubbles or dendrimeres. In fact, they are characterized by chemical and geometric tunability and ability to interact with biomolecules to facilitate uptake across the cell membrane. Moreover, nanoparticles can increase the bioavailability, solubility and permeability of many potent drugs. Finally, they also reduce the drug dosage frequency and increase the patient compliance[7].

1.3 Myocardial Regenerative Medicine

Ischemic heart disease (IHD) is characterized by insufficient supply of blood and oxygen to the heart muscle caused, especially from atherosclerosis, a cholesterol plaque that reduces the diameter size of the lumen of the blood vessel. IHD is the leading single cause of mortality worldwide. In Europe, it is responsible each years for 18% of all deaths among man and 20% as regard women[8]. Almost 700,000 people die of heart

disease in the U.S. every year (29% of all deaths), of which approximately 3% suffer from myocardial infarction (MI) annually[9].

MI is the process of cell death occurring after the obstruction of one or more branches of the coronary arteries that determine the blockage of blood flow to the cardiac district and the consequent necrosis of cardiac muscle tissue within 20-40 minutes after the occlusion. Repair of the infarcted myocardium can be divided into three different phases (Figure 1): the inflammatory, the proliferative and the maturation phase[10]. In all three phases of infarct healing, the cellular responses that mediate cardiac repair is influenced especially by the dynamic changes in the composition of the extracellular matrix (ECM).

The inflammatory phase (1-7 days) starts after a massive cardiomyocyte death (up to 11 billion cells), apoptosis or necrosis, to the decreased oxygen supply and commences already 4 hours after the MI. This phase creates a favorable environment to allow the reparation of the cardiac tissue, removing the dead cells by macrophages action. Macrophages are important cells of the immune system which, beside the phagocytosis, they induce cytokine and chemokine expression causing marked infiltration of the infarcted tissue with neutrophils and mononuclear cells[11]. So, cytokine activations determine the fibroblasts recruitment in the infarcted area. Another important macrophages function is the secretion of proteolytic enzymes which degrade and reshape the existent matrix. Moreover, the macrophages induce release of anti-inflammatory mediators, including Transforming Growth Factor (TGF)-β, Interleukin (IL)-10 and pro-resolving lipid mediators (such as the lipoxins, resolvins, protectins and maresins)[11]. The first phase is characterized by thinning of the ventricle wall, stiffness increasing and loss in contractility. The repression of pro-inflammatory signals and the immune cell recruitment in the damaged area of the heart, mark the transition to the proliferative phase of infarct healing.

During this second phase (7-28 days), the infarct is infiltrated with abundant fibroblasts and vascular cells. The dynamic alteration of the ECM in the proliferative phase provides essential signals for conversion of fibroblasts into myofibroblasts, activating angiogenic pathways necessary for formation of new vessels, and supplying the oxygen, nutrients and growth factors[10]. Activated myofibroblasts secrete collagens and other matrix proteins, causing granulation tissue formation which replaces the lost cardiomyocytes, but it causes mechanical and structural properties alteration. Finally, during the maturation phase (18-56 days), the ECM crosslinking lead to formation of a stable collagen-based scar tissue. Although, the scar tissue preserves the ventricle

integrity, it results fibrotic and poor vascularized and it possess minor contractility and electrical conduction compared to the cardiac tissue[6].

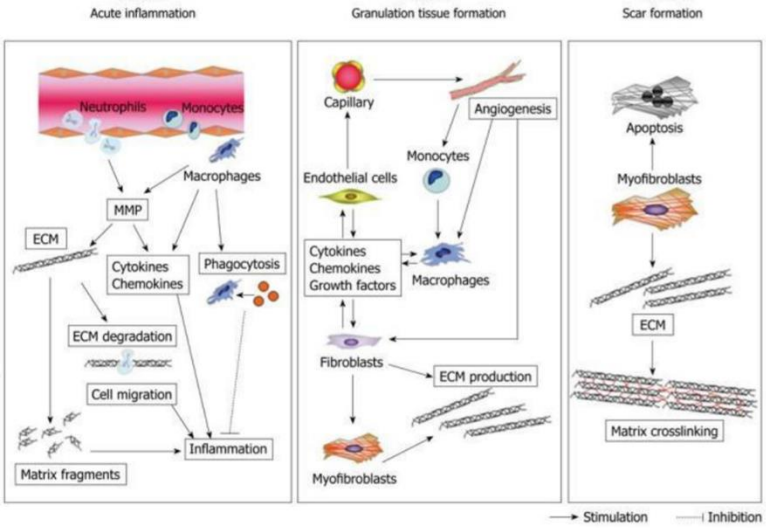

Figure 1 *Phases of cardiac healing and remodeling after myocardial infarction*

1.3.1 The clinical problem and the available treatment approaches

The goals of traditional therapies are pain relieve, reduce heart workload and prevent/resolve complications post infarct. To achieve these purposes there are mainly two possible approaches: the pharmacologic and surgical approaches. The first is based mainly on thrombolytic, anticoagulant and antiplatelet therapy, β-blockers and nitrates. The second approach is divided in two ways (Figure 2): percutaneous transluminal coronary angioplasty (PTCA) and coronary artery bypass graft (CABG).

PTCA used coronary stents, inserted by catheters, to restore the lumen of the vessel. Instead, CABG is a surgical procedure to restore normal blood flow to an obstructed

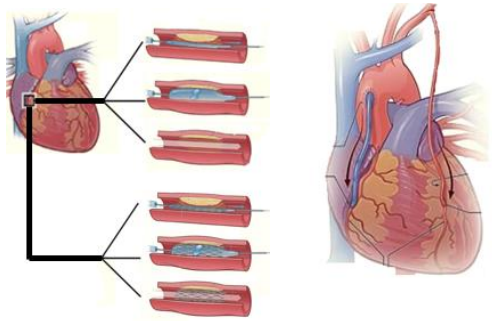

Figure 2. *percutaneous transluminal coronary angioplasty-PTCA (left) and coronary artery bypass graft- CABG (right)*

coronary artery. The blocked artery is 'bypassed' by sewing (grafting) another blood vessel to the aorta at one end and to the coronary artery beyond the damaged area the other end.

Although, in the last decades many efforts have been dedicated on improving treatments during the acute phase of the myocardial infarction and enhancing the contraction of the surviving myocardium, none of these approaches are aimed at inducing the formation of new functional cardiac tissue. Currently, transplantation remains the only therapeutic option for end-stage heart failure [12]. However, the restrict number of organ donors limits the access to transplantation to a few patients each year[13]. Moreover, the administration of anti-rejection immunosuppressive therapy is needed for the rest of life[14].

Therefore, it is clear the need of developing alternative strategies to treat heart failure patients. In this context, extraordinary efforts have been devoted towards the identification of novel approaches to induce heart regeneration.

1.3.2 Novel regenerative therapies

Heart regeneration has been intensely investigated, and extremely controversial, for over century[15]. Although, at the beginning it has been doubted whether the heart can grow by multiplication of myocytes[16], recently, the adult human heart is no longer considered a static organ unable to replace its parenchymal cells during the course of life[17].

To date, the understanding of the process of myocardial regeneration, in particular after an ischemic damage, is currently under debate. Moreover, the adult human heart has a limited capacity to regenerate lost or damaged cardiac myocytes following cardiac insult[16] [18]. Indeed, the myocardial injury is characterized by excessive fibrosis and cardiac remodeling, leading to disproportionate thinning of the heart wall and severely impaired cardiac structure and function[6]. This impairment of the heart's ability to pump blood has disastrous consequences on morbidity and mortality[3].

The aim of the strategies for the reparation of cardiac tissue is to stimulate myocardial regeneration by inducing self-repair processes, improving tissue recover, reversing or attenuating adverse remodeling, and, ultimately, achieving long-term stabilization and improvement in heart function. Five major processes associated with MI are being therapeutically targeted at present by various experimental strategies to reduce the fibrosis: cardioprotection, inflammation, vascularization, remodeling fibrosis and

cardiomyogenesis. The last solution, unlike the other, is a regenerative strategy that aims to repair the infarcted area through two possible way: cell therapy (exogenous regeneration) and endogenous regeneration [14].

1.3.2.1 Cell therapies

Cell-based therapies using different type of cells have been proposed with the aim to regenerate the infarcted area by injecting or engrafting cells locally into the infarcted tissue. The goal is to repopulate damaged area of myocardium with functional cells that restore the cardiac function, enabling sufficient oxygen and nutrient circulation to all the vital organs of the body.

Several adult stem (cardiac progenitors cells, endothelial progenitor cells and skeletal myoblasts) and cardiac myocytes derived from induced pluripotent stem cells (iPSCs)or embryonic stem cells (ESCs) have been proposed as possible solutions[6].

Adult stem and cardiac progenitor cells:

Adult stem cells (Figure 4) are self-renewing, clonogenic and multipotent cells with the ability differentiate into cell types of the tissue in which they reside and often to differentiate into cells of other types of tissues.

The use of adult stem cells avoids ethical problems of the ESCs and has two additional advantages: (i) they can be isolated from patients, overcoming the problem of immunological rejection and (ii) the risk of tumor formation is significantly reduced compared to the use of embryonic stem cells[19].

Despite a remarkable plasticity in differentiation potential of stem cells derived from adult tissues was recently suggested transdifferentiation [20], this concept remains controversial.

The regenerative approach based on Adult stem cells has attempted different cell types either alone[21] (Skeletal myoblasts, Bone Marrow Stem cells, Endothelial progenitor cells, Myocardial stem cells) or in combination [22] (Figure 4).

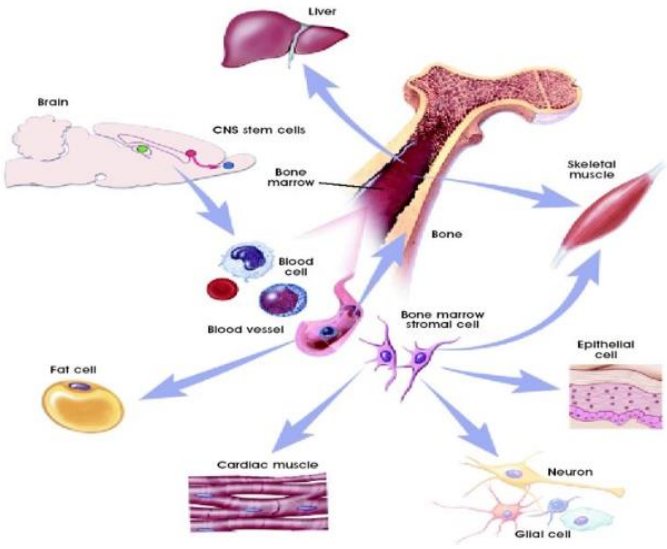

Figure 3 *Adult stem and progenitor cells transdifferentiation*

Skeletal myoblasts:

Skeletal muscle-derived myoblasts, easily obtainable from patient biopsies, are sited between the basal lamina and sarcolemma and account for 2–5% of sub-laminar nuclei of mature skeletal muscle. They are characterized by high proliferative potential *in vitro*, maintaining their undifferentiated status, high resistance to ischemic stress, low risk of tumorgenicity and autologous availability[22].

Animal models suggest that skeletal myoblasts have a remarkable effect in improving ventricular functions in MI [23]. However, their application in clinical trials has been limited by severe arrhythmias, maybe correlated to the lack of functional electrical coupling between skeletal muscle and cardiomyocytes[24].

Endothelial progenitor cells (EPCs):

Endothelial progenitor cells (EPCs) are circulating endothelial progenitors derived from bone marrow. They express some typical stem cell markers such as CD34, CD133, and VEGF-Receptor-2 (VEGFR-2). Animal models of cardiac ischemic injuries have showed that intramyocardial transplantation of autologous EPC may represent a practical approach to promote the revascularization in patients with chronic myocardial ischemia[25].

As it can be seen by numerous clinical studies, intramyocardial transplantation of adult stem and progenitor cells in the post-infarct myocardium induces neoangiogenesis and promotes cardiomyocyte survival, reducing the infarct size and improving cardiac

function long term. However, no study highlights cardiomyogenesis effect[26]. Moreover, the low accessibility and proliferation capacity have actually limited the use of adult cells in the treatment of cardiovascular diseases [24].

Cardiac Progenitor Cells

More recently, new scientific studies have made use of cardiac progenitor cells (CPCs) as promising candidate for cardiac regeneration[27].

CSPs have been isolated from their "resident niche" and expanded in an in vitro, and subsequently they are transplanted into the damaged hearts of patients. The principal advantages linked to CPCs are their differentiation potential and the ability to produce and remodel ECM proteins. The cell therapy approach generally used to treat a myocardial infarction is based on isolation and expansion *in vitro* of CPCs and their transplantation into the infarcted area. This regenerative approach has shown immediate benefits on cardiac function, nevertheless this treatment has exhibited very limited improvement on the long term, because to low cell survival and engraftment in the host tissue. Indeed, a myocardial infarction generates a hostile environment for the injected progenitor cells, due to the inflammatory response and tissue alterations, such as scar tissue formation, triggered by the cardiac injury[28].

Embryonic stem cells (ESCs):

Embryonic stem cells (ESCs), which are derived from the inner cell mass of mammalian blastocysts[24], have the ability to replicate indefinitely while preserving pluripotency. Moreover, they are able to differentiate into cells of all three germ layers: endoderm, ectoderm and mesoderm[29]. Therefore, ESCs have the potential to completely regenerate the myocardium.

Human ESC-derived cardiomyocytes exhibit early cardiac transcription factors (e.g. Nkx2.5), as well as the expected sarcomeric proteins, ion channels, connexins and calcium-handling proteins. They show functional properties comparable to those expressed by cardiomyocytes in the developing heart, and they undergo similar mechanisms of excitation-contraction coupling and neurohormonal signaling[15].

However, their use for regenerative therapy is hampered, by ethical controversy, by immunological rejection and potential tumorgenicity when injected *in vivo*[30].

Induced pluripotent stem cells (iPSCs):

Induced pluripotent stem cells (iPSCs or iPS) were originally created by the reprogramming of adult somatic cells (e.g. skin fibroblasts) through the forced

expression of up to four stem cell associated transcription factors (Oct4, Sox2, Klf4, and c-Myc)[15].

The iPS cells may overcome two important limitations of ES cells: ethical concerns about harvesting ES cells from embryos and graft rejection by the patient's immune system, because iPS cells can be custom engineered from a patient's stromal cells for autologous transplantation[31].

The "first-generation" iPSCs were generated introducing integrating viruses as reprogramming factors[29], with consequent associated risk of neoplastic conversion[31]. Recently, alternative reprogramming strategies have been proposed to reduce or eliminate the risk of neoplastic conversion, such as the use of episomal gene delivery, excisable transgenes, synthetic mRNA, cell-permeant recombinant proteins[15] and small molecules[31].

iPSCs represent a potentially inexhaustible supply of human cardiomyocytes. Consequently, in the last decades, their use as source for heart regeneration has been deeply studied[32].

For example, Lei Yang's laboratory repopulated decellularized mouse hearts with human iPS cell-derived multipotential cardiovascular progenitor cells, creating an engineered cardiac tissue. The work demonstrated *ex vivo* proliferation, migration, and differentiation of its into cardiomyocytes, smooth muscle cells in a 2D scaffold and endothelial cells. However, the mechanical force generated by engineered heart tissues was insufficient for pumping blood like the native heart and the whole engineered constructs were not fully synchronized[33].

In the study by Guyette et al. a decellularized human heart was repopulated with cardiomyocytes derived from nontransgenic human IPS cells. This work demonstrated that the cardiomyocytes adequately engrafted onto the cardiac scaffolds and showed electrical conductivity, providing a foundational toolset to generate patient-derived human myocardium for future works[34].

Indeed, further studies are needed before this technique can be translated into clinical applications [32].

1.3.3 Therapies enhancing endogenous regeneration

Despite, the adult human heart has a limited regenerative ability, the observation that the postnatal heart retains some proliferative capacity has inspired therapeutic approaches that aim to enhance the endogenous cardiomyocyte proliferation for regeneration.

More precisely, the endogenous strategy aims to recruit pre-existent autologous cells of the patient in order to repair the heart.

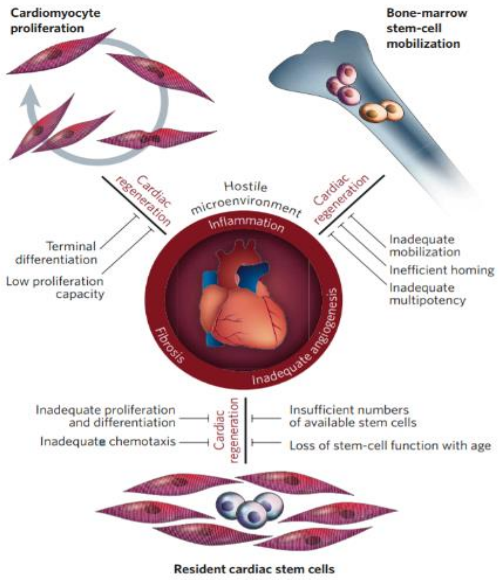

Figure 4. *Endogenous cell therapy*

Three main pathways for new cardiac myocyte generation have been proposed (Figure7): (i) division of preexisting mature cardiac myocytes (CSCs), (ii) amplification of dedifferentiated cardiac myocytes and (iii) differentiation of progenitor cells (from bone marrow)[31][12].

1.3.3.1 The therapeutic target of approaches for endogenous regeneration

Resident cardiac stem cells (CSCs)

The stem cells reside in a microenvironment called niche, within which stem cells maintain their undifferentiated state and obtain growth signals from the supporting cells. Stem cells can divide symmetrically or asymmetrically depending on the signal received, generating new stem cells and cells fated to acquire specific functions[17][35].

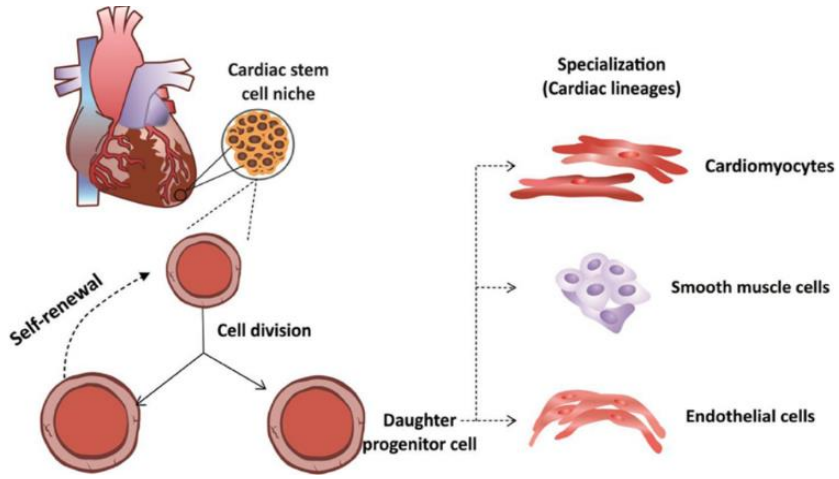

Figure 5 *Resident cardiac stem cells (CSCs)*

Many researches indicated that adult mammalian myocardium contains a population of resident cardiac stem cells (CSCs,) with the differentiation ability[36]. Beltrami et al. (2003) were the first to isolate CSCs. Moreover, they demonstrate that this population of cells is positive for the c-kit surface receptor[16].

Finally, CSCs revealed clonogenic and self-renewal capacities and multipotentiality, allowing them to differentiate along the three main cardiac lineages: myocytes, endothelial cells and smooth muscle cells[35][37][38].

Beltrami's work was confirmed later by Smith et al.[39] that demonstrated the CSCs ability to differentiate *in vitro* and *in vivo*.

According to Urbanek's work[37], CSCs are distributed throughout the heart, assuming the possibility that those located within the infarct or in its proximity could divide and differentiate reconstituting damage myocardium area.

Therefore, CSCs seem to be the most logical cells source to exploit for cardiac regeneration therapy. Their presence into the heart, the recurrent co-expression of early cardiac progenitor transcription factors, and the capability for *ex vivo* and *in vivo* differentiation into cardiomyocytes might reduce infarct size, improve function, and decrease mortality[21].

Despite many studies have been developed regarding CSPs, nowadays, the real regenerative effect of the adult cardiac stem cells in myocardial infarct is still unknown. Accordingly, the intramyocardial injection of c-kit– positive CSCs or their local activation by growth factors results in significant reconstitution of the infarcted heart[18][40]. However, other works suggest that CSCs apoptosis during the myocardium infarct results in a high decline of the number of functionally competent

CSCs. This might explain the inability of CSCs to migrate and reach the necrotic area and their incapacity to form myocytes and coronary vasculature that may counteract the chronic loss of parenchymal cells and vascular structures, as demonstrated in Urbanek's work[37]. Moreover, without considering the infarct, myocyte apoptosis increases linearly with age[17] and this might explain the less regenerative power of myocardium in elderly subjects suffered from post-infarct ischemic heart disease[40].

In conclusion, the CSCs appear to be properly equipped to regulate tissue homeostasis, although their potentiality is insufficient to regenerate tissue has not been established yet in ischemic injury or, late in life, in aging and senescence of the organ[17].

Cardiomyocytes proliferation

Regeneration of cardiac damage is limited because of the low proliferative potentiality of cardiomyocytes during adult life.

Cardiomyocyte proliferation has an important role in the regeneration of the heart in some vertebrates, but the proliferative capacity of these cells is limited in the adult mammalian heart.

Despite some studies revealed that human cardiomyocytes have a turnover rate during the human live[26] and that there is myocyte proliferation and division after myocardial infarction[16], However, the level of proliferation is insufficient to regenerate the lost tissue (0.45%-1% per year)[26].

Bone-marrow-derived cells

Another exogenous approach that has been proposed is the mobilization of bone-marrow cells (Figure 9) in the heart infarcted area. The adult bone marrow contains several cell populations. In addition to differentiated cells, such as stroma cells, vascular

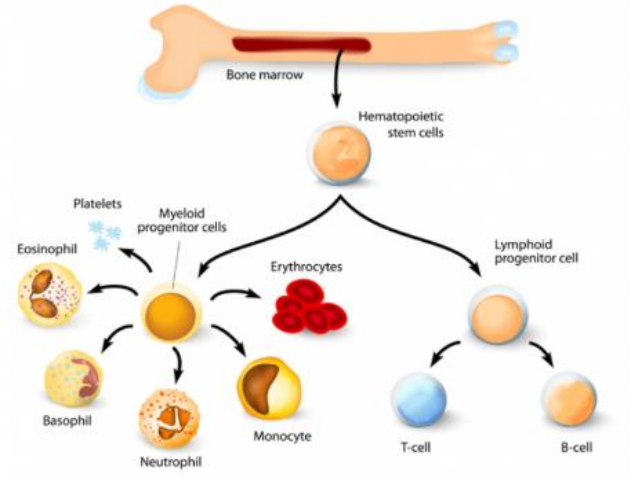

Figure 6. *Bone-marrow derived cells*

cells, adipocytes, osteoblasts, and osteoclasts, primitive and progenitor cells reside in the bone marrow[41]. The first evidence that adult bone-marrow-derived progenitor cells could participate in the formation of cardiomyocytes in adult human hearts was based on reports of Y-chromosome-positive cardiomyocytes in female donor hearts transplanted in male recipients[42].

However, this strategy was unsuccessful for three reasons. First of all, the studies in the last decade have not demonstrated differentiation of hematopoietic progenitor cells into cardiomyocytes or improvement in cardiac function[41] [30]. Secondly, bone-marrow cells are present in low quantity in the blood, so they have to recruited in the infarct area with specific drugs or devices. Lastly, the fibrotic, inflamed and poor vascularized infarct area makes difficult the bone-marrow cells survival.

However, It has been demonstrated that, despite bone-marrow-derived hematopoietic cells (HSCs) and marrow-derived stromal cells (MSCs) are enable to differentiate directly into new cardiomyocytes, they manage through paracrine release of cytokines to control the response of cells native to the myocardium, and thereby regulate healing. Therefore, they result useful for the angiogenic regulation, cardiomyocyte survival, and left ventricular remodeling post-infarction[15] [31] [30]. For these reasons HSCs and MSCs has been used as first adult stem cells in exogenous therapy in clinical transplantation [32].

1.3.3.2 Bioengineering approaches for cardiac regeneration based on scaffolds and hydrogels

Even though stem cell-based therapy have been used for clinical applications, showing some benefits, cell transplantation into the infarcted cardiac area has limitations connected to low cell survival, engraftment rates and increase of arrhythmia[43]. Another strategy used for regeneration of hearts is the delivery of growth factors (e.g. vascular endothelial growth factors). However, bolus injection of growth factors into the infarcted area showed some limitations such as fast release profiles of growth factors and biochemical instability. To overcome these limits of stem cell and growth factor therapies, scaffolds have been used for increasing the engraftment rate in the infarcted area and delivery efficiency. Scaffolds are materials that have been engineered to cause desirable cellular interactions to contribute to the formation of new functional tissues for biomedical purposes. Several types of scaffolds have been proposed in cardiac engineering, including cardiac patches and injectable hydrogels, as vehicle for the delivery of cells and growth factors[44].

Three-dimensional dermal fibroblasts have been used in cardiac patch by Kellar et al. [44]; Piao et al. [7] applied stem cell-seeded poly-glycolide-co-caprolactone scaffolds to a myocardial infarction; whereas Shimizu and colleagues made a cell-based cardiac sheet without an artificial scaffold[45].The slow release of growth factors in a gelatin hydrogel has been demonstrated to improve heart functions, and photocrosslinkable chitosan-based hydrogel has been applied to infarcted animals.

The regeneration of infarcted heart can also promoted by applying into the infarcted tissue, an empty scaffold (without cells or growth factors inside the scaffold) that is able to recruit cells from the surrounding tissue. Indeed, Robinson et al.[44] realized a left ventricular wall patch using the urinary bladder matrix (UBM), applying successively in a porcine infarction model.

This promising technique seems to have the ability to regenerate the damaged area avoiding possible side effects of stem cells and growth factors. because only scaffolds could determine the alteration of the microenvironments in the infarcted heart.

Another particular type of scaffolds used recently in tissue engineering are the Hydrogels. They are hydrophilic polymer networks which may absorb from 10–20% up to thousands of times their dry weight in water. Hydrogels may be chemically stable or they may degrade and eventually disintegrate and dissolve. Moreover, they could have pores large enough to accommodate living cells, or they may be designed to dissolve or degrade, releasing growth factors and creating pores into which living cells may penetrate and proliferate[46].

Hyaluronic acid (HA) is an encouraging material for hydrogels. It is an unbranched glycosaminoglycan polymer of two repeating units and largely distributed in the extracellular matrix. The different biological activities of hyaluronic acid, including promoting angiogenesis, inhibiting cell adhesion and suppressing fibrous tissue formation, depend on the molecular weight [45]. S.J Yoon' s work[45] showed that injectable hyaluronic acid-based hydrogels without stem cells and growth factors has been used to regenerate heart muscles in an infarcted area, showing cardiac function recovering, such us contractility and diastolic and systolic function.

1.3.4 An innovative approach: Direct reprogramming of cardiac fibroblasts into cardiomyocytes

In the last few years, researchers focused started to study an innovative approach for cardiac regeneration based on the direct conversion of the cardiac fibroblast population into cardiomyocytes, by direct reprogramming the scar tissue of the cardiac scar tissue.

Cardiac fibroblasts are somatic cells, completely differentiated cells without cardiogenic potential but only structural functions. Cardiac fibroblasts secrete biochemical signals and contribute to the scar formation in the cardiac injury[5]. They represent the most prevalent cell type in the adult human heart and are the principal mediators of cardiac fibrosis and scar formation post-MI[47].

The possibility to reprogram endogenous cardiac fibroblasts directly into cardiomyocytes with the introduction of precise biochemical factors without passing through the differentiation of pluripotent stem cells, offers an alternative approach and implicates many therapeutic aspects. First of all, the risk of tumor formation caused by the introduction of stem cells can be reduced. Secondly, patient-derived fibroblasts (present in huge amount) can be taken through skin biopsy, grown *in vitro* and delivered successively to damaged heart. Finally, the direct reprogramming of the scar tissue could easily contribute to the overall contractility of the cardiac muscle[5]. Therefore, cellular reprogramming holds tremendous potential for promoting such cardiac repair. This new regenerative strategy has been recently achieved by specific combinations of lineage-significant transcription factors (GMT: Gata4, Mef2c, and Tbx5)[48] or microRNAs (miRNAs) or small molecular [6].

In 2013, Nam et al.[47] showed that cardiac marker expression can be activated by the combination of GATA4, HAND2, TBX5, MYOCD (myocardin), miR-1, and miR-133, however the majority of these induced cardiomyocytes were not in a totally reprogrammed state. In the same period, Wada and colleagues[49] found out that the transcription factors GATA4, MEF2C, TBX5, MESP1, and MYOCD (GMTMM), used for reprogramming fibroblasts, could change the cell morphology and exhibited spontaneous Ca2+ oscillations. Srivastava et al. [49] revealed that reprogramming of human fibroblasts into cardiomyocytes was insufficient with GMT, but, adding ESRRG and MESP1, it could be possible to realized cardiomyocyte-like cells that expressed specific cardiac gene and sarcomere-like structures. Moreover, the addition of MYOCD and ZFPM2 helped to obtain more features of cardiomyocytes as well as a phenotypic shift to a cardiac state and a global cardiac gene expression.

The combination of miRNAs, called “miR-Combo” (miRNAs 1, 133, 208, and 499) is able to redirect *in vitro* and *in vivo*, non-cardiac myocytes into cardiomyocyte-like cells (iCMs) [3].

Jayawardena’s work showed that the fibroblasts reprogramed in vitro through the miR-Combo, possessed functional properties typical of cardiac myocytes such as L-type channel expression, spontaneous calcium oscillations and contractility[50], besides an important improvement of the cardiac function following myocardial infarct. However,

their physiological properties seemed to be less mature when compared to neonatal cardiac myocytes[3].

In conclusion most direct reprogramming experts have been could out on mouse cell. Reprogramming of the human cells was also attempted, ordering the need for a wider combination of transcriptional factors, miRNAs or small molecular aspect to mouse cells. Overall reprogramming efficiency is still for a clinical application.

1.3.4.1 microRNA biology

MicroRNAs (miRNAs) are small non-coding RNAs (20–24 nucleotide long) belonging to a class of small silencing RNAs that are extremely important in the post-transcriptional regulation of genes. Recently, the key role of miRNA have been demonstrated, such as the regulation of wide range of biological functions, including cell survival, differentiation, proliferation, metabolism, apoptosis, tumor growth, and metastasis, besides indirect and direct reprogramming to multiple lineages[6].

miRNA genes are transcribed by RNA polymerase II (Pol II), and the long primary transcript has a local hairpin structure where miRNA sequences are embedded[51]. The resulting transcript, known as primary-miRNA (pri-miRNA), is ~1000 nucleotides in length, possesses a 5′cap, a middle stem loop structure, and a 3′ polyadenylated tail[6]. Pri-miRNAs are processed into pre-microRNAs by the RNA-processing complex (Microprocessor complex) formed by Drosha and DGCR8. Drosha cleaves the 5′cap and 3′ poly (A) tail leaving a ~65bp stem loop structure containing the mature miRNA. Following cleavage by Drosha, the pre-miRNA is transported from the nucleus into the cytoplasm by Exportin 5, a protein that, in humans, is encoded by the XPO5 gene. Once in the cytoplasm the pre-miRNA is cleaved further by the RNase III-type endonuclease Dicer (Double-Stranded RNA-Specific Endoribonuclease) into a smaller fragment (18 ~ 25 nt) containing the mature miRNA duplex. The pre-miRNA, successively the processing by Dicer, is bound by an Argonaute protein, and incorporated into an RNA-induced silencing complex (RISC) that utilizes the microRNA to identify and silence its target genes.

The core of the RISC complex is comprised of two components: an Argonaute protein (Ago1-Ago4 in mammals) and a GW182 protein (TNRC6A-C in mammals). While Ago proteins bind to miRNAs and are thus involved in target recognition, GW182 proteins seem to act as a molecular platform to which effector complexes bind to mediate target repression[52]. A Schematic representation of the biogenesis of miRNA could be seen in Figure 10.

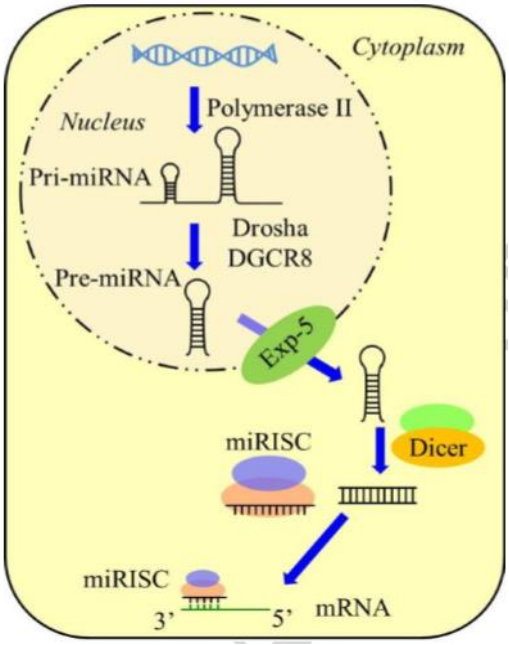

Figure 7. *Schematic representation of the biogenesis of miRNA*

1.3.4.2 MicroRNAs in direct reprogramming of fibroblasts into cardiomyocytes

To date, several miRNAs have been shown to be crucial for cardiac differentiation. Their importance in cardiac development has been confirmed by evidence from various studies[6] [3] [50]. A subgroup of miRNAs, known as myomiRs or muscle-specific miRNAs (Figure 11), plays an important role in muscle differentiation, survival, and proliferation. The myomiRs miR-1, miR-133, miR-208a, miR-208b, and miR-499 are the main regulators of proliferation, survival, and differentiation of cardiac precursors. miR-1 and miR-133 are highly expressed in both heart and skeletal muscle and they are implicated in the control of cardiac cell fates and in cardiac conduction system, whereas miR-208 and miR-499 regulate the expression of myosin[53].

miR-1 has been proved to induce cardiomyocytes differentiation and anti-proliferative effect. Through the repression of histone deacetylase 4 (HDAC4), which negatively regulates Mef2, miR-1 inducts the myogenic phenotype, whereas the anti-proliferative function is linked to repression of Hand2, a transcription factor involved in cardiomyocyte proliferation. miR-1 has been demonstrated to elicit pro-apoptotic responses in cardiomyocytes, as well as in other cellular systems. Indeed, the miR-1 overexpression was tested in mice and the results showed the loss of cardiomyocytes and inducing of a lethal cardiac hypoplasia, while its deletion led to altered cardiogenesis with consequent failure in ventricular septation and immediately death in few hours after birth. miRNA-1 has been also shown to have a role in apoptotic cell death because the repression of the anti-apoptotic proteins BCL2 and IGF. Furthermore, it plays a key role in cell electrophysiology control, with potassium as well as pacemaker channels as direct targets. Finally, miR-1 up-regulation upon MI seems to be responsible for the higher risk for arrhythmias in MI patients, in fact the blockade of miR-1 upregulation reduces arrhythmias correlated to MI.

Also, miR-133 been shown to be involved in cardiomyocyte proliferation because it directly represses cyclin D2. Complete ablation of miR-133 causes cardiac defects during embryogenesis showing dilated atria, and an enlarged heart containing thrombi[24].

Under physiological conditions the heart are abundantly expressed three important miRNAs: miR-499, miR-208a, and miR-208b, which are embedded in the introns of three myosin genes: miR-208a in α-MHC (also known as Myh6), miR-208b in β-MHC (Myh7), and miR-499 in Myh7b genes.

miR-499 has a negative effect on cardiomyocyte apoptosis, indeed it inhibits two pro-apoptotic proteins involved in the mitochondrial fission program, isoforms of the calcineurin catalytic subunits (CnAα and CnAβ) and dynamin-related protein-1 (DRP1). It has been shown that knockdown of miR-499 in mice potentiated apoptosis, upon ischemia/reperfusion (I/R), determines a rise of myocardial infarct size, and decrease of cardiac function, whereas miR-499 transgenic mice presented a smaller infarct size and less apoptosis compared to controls. Furthermore, miR-499 plays also a key role in the increase differentiation of cardiac stem cell into cardiomyocytes with mechanical proprieties like native cardiomyocytes, thus allowing myocardial mass restoration and function in the infarcted heart.

miR-208a has been demonstrated to have a key role in cardiac hypertrophy linked to stress, operating on thyroid hormone receptor associated protein 1 (THRAP1) and in the regulation of the myosin heavy chain (MHC) isoform switch (from alpha to beta) during

physiological and pathological conditions. Studies proved that miR-208 induces not only cardiomyocyte hypertrophy and fibrosis but also it is required for the hypertrophic growth under stress. Instead, the role of the co-transcribed miR-208b in human hypertrophy must be clarified[24].

Adopting a combinatorial approach, it was identified that the combination of miRNA-1, miRNA-133a, and miRNA-208a induced the expression of early markers of commitment to the cardiomyocyte lineage. Furthermore, the addition of miRNA-499 further augmented the efficiency of cardiac reprogramming[6]. This combination is said miR-combo and a single transient transfection may induce the expression of cardiac markers (such as Mef2C and αMHC) in mouse fibroblasts, as well as the formation of, organized sarcomeres, contraction, and spontaneous calcium transients approximately 4 weeks after transfection, as can be seen in the H.Kim's study[53].

In the Jayawardena's study, the results demonstrated that miR-combo can induce: (i) the *in vivo* reprogramming of non-cardiac myocytes in the heart to cardiomyocyte-like cells with morphological and functional properties similar to those of mature adult ventricular cardiac myocytes; and (ii) a significant improvement in cardiac function following myocardial infarct[3].

Therefore, the use of microRNAs represents a promising alternative strategy for direct reprogramming of fibroblasts into cardiomyocytes that may overcome some of the limitations encountered using viral vector, allowing administration though non viral vectors [50].

1.4 Design of microRNA delivery vehicles

The main obstacle to the progression of miRNA therapy is the realization of vehicles with the ability to maintain the stability and integrity of oligonucleotides in circulation. Naked miRNAs are characterized by poor cellular uptake and they are degraded within seconds by the abundant nucleases such as serum RNase A-type nucleases present in the blood. Moreover, naked miRNAs are cleared rapidly via renal excretion, leading to a short half-life in systemic circulation[54]. Then, the successful application of miRNA largely depends on the development of effective delivery platforms. Besides the obvious requirements of low cytotoxicity and high transfection efficiency, an ideal miRNA delivery vehicle for regenerative medicine need to be biocompatible, non-immunogenic, biodegradable and able to deliver the miRNA at specific tissue or organ in a local and sustained manner. Viral vectors have been extensively used. However oligonucleotides such as synthetic miRNA mimics, antimiRNA and siRNA can be also conjugated or

complexed with nanocarriers, which renders them more resistant to nuclease degradation when compared with free oligonucleotides[55]. Thus, numerous viral and non-viral vectors with high transfection efficiency, good biocompatibility, and even high targeting efficiency have been developed for miRNA delivery.

1.4.1 Viral vectors

Several viral vectors such as retrovirus, adenoviruses, lentiviruses and adeno-associated viruses (AAVs) are used today to deliver vectors encoding miRNAs into the cell nuclei and efficiently express miRNAs. The advantages of using viral vectors are their natural ability to enter the cells and express their own proteins, as well as their high transduction efficiency, high transfection rate and sustained transgene expression of viral vectors. All this renders them attractive for oligonucleotides delivery both *in vitro* and *in vivo*.
However, the use of viruses in gene therapy could be limited by various factors. First of all, security issues have been raised following the death of a patient during a clinical trial that investigated the potential of gene therapy using viral vectors. Secondly, viruses present many potential disadvantages linked to the patients such as toxicity, immune responses, inflammatory responses, low loading capacity and quality control. Lastly, insertional mutagenesis and oncogenic effects and cancer formation can occur when used in vivo[54].
The limitations of viral vectors in clinical applications has led to the evaluation and development of alternative vectors based on non-viral carriers, such as polymer or lipid, for a safer and more manufacturable delivery systems in miRNA therapy.

1.4.2 Non-viral vectors system

To overcome such limitations, non-viral miRNA delivery systems, such as polymeric nanoparticles, liposomes, polymeric micelles and dendrimers have been proposed. These delivery systems protect the degradation of miRNAs by nucleases and increase their half-life in the blood, can escape from endosomal and/or lysosomal degradation, and deliver miRNAs to the cytoplasm or nucleus.
Despite non-viral delivery systems usually show lower transfection efficacy and shorter duration of target gene expression compared to viral vectors, recent studies successfully demonstrated that non-viral carriers with rational design and suitable modifications can also achieve clinically relevant efficiency[54].

1.4.2.1 Nanoparticles as microRNA delivery systems

Nanoparticles are submicron-sized colloidal spherical particles able to carrier a therapeutic agent of interest by encapsulation within their matrix, adsorption or conjugation onto their surface[7]. Moreover, they are capable of targeting at several levels from organs to tissue and cells. Targeting can be achieved by applying external stimuli, like ultrasounds or magnetic fields, or by simply taking advantage of the size of the carriers (passive targeting) which could be tuned in order to enable nanoparticles to leak through peculiar vasculature fenestrations of different organs and tissues[56]. For these reasons the nanoparticles are largely used as delivery system.

Appropriate method and materials for the preparation of nanoparticles are chosen depending on the type and quantity of the desired drug. The main manufacturing methods for the formation of nanoparticles includes solvent evaporation, nanoprecipitation techniques, emulsification and salting out [26]. They are described briefly below.

• Solvent evaporation

The polymer is dissolved in a volatile organic solvent such as dichloromethane, chloroform or ethyl acetate. The emulsion between polymer solution and aqueous phase, obtained with high speed of homogenization or with ultrasonication, is converted into nanoparticles by the evaporation of solvent, which takes place either with magnetic stirring or under reduced pressure or by increasing the temperature. Subsequently the nanoparticles can be ultracentrifuged and washed with distilled water to remove any additives, such as surfactants, and finally lyophilized.

• Nanoprecipitation (solvent displacement method)

It is the precipitation of a polymer preformed from an organic solution and diffusion of the organic solvent in an aqueous medium, with or in the absence of a surfactant. The deposition at the interface between water and organic solvent causes a rapid diffusion of the solvent and formation of a colloidal suspension. A commonly used solvent is acetone, which is miscible in water and easily removed by evaporation. It is a widely used method both for the preparation of nanocapsules and nanospheres.

• Emulsification

It is a modification of the method of evaporation of the solvent, which is eliminated by evaporation or filtration, according to its boiling point. A water-soluble organic solvent, such as acetone and methanol, is interfaced with an insoluble one such as

dichloromethane and chloroform. The spontaneous diffusion of the first in the second creates an interfacial turbulence between them and the formation of smaller particles

• Salting out

It consists in the separation of a water-miscible solvent from an aqueous solution, by salting out. The polymer and the drug are dissolved in a solvent, such as acetone, then emulsified in an aqueous gel containing a stabilizing colloid and the salting out agent, the choice of which is fundamental for the drug encapsulation efficiency. The salting out agent and the solvent are then eliminated by crossflow filtration.

Later we treated two typical material classes present in literature for the realization of nanoparticles that allow the loading and release of miRNA in cardiac engineering: lipids and polymers.

1.4.2.1.1 Lipid-based nanoparticle delivery systems for miRNA delivery

Lipid-based nanoparticles (LNPs) such as liposomes, solid lipid nanoparticles (SLN) and nanostructured lipid carriers (NLC) have received great attention during the last decade. These nanoparticles can transport hydrophobic and hydrophilic molecules, exhibit really low toxicity, and increase the time of drug action implicating a prolonged half-life and a controlled drug release. Furthermore, lipid nanosystems can be modified chemically to avoid the detection by the immune system (gangliosides or polyethylene glycol (PEG)) or to increase the solubility of the drug [57].

Due to their relative simplicity, biocompatibility and biodegradability property, LNPs have been widely used in systemic delivery of siRNA and miRNA as nanocarriers. LNPs can protect nucleic acids from enzymatic degradation, simplify the cellular uptake and increase the circulation half-life time of oligonucleotides[56].

Generally, cationic lipids, neutral lipids and PEG-lipids or a mixture thereof can be used to form lipoplexes for miRNA delivery.

Cationic liposomes and lipoplexes were the first positively charged delivery devices to be investigated and were found to have a good degree of transfection[58]. These lipids are characterized by a cationic head group and a hydrophobic moiety attached by a linker[55]. The electrostatic bonding between positively charged head group and nucleic acid phosphate groups creates a complex with a net positive charge which interacts with negatively charged cell membranes, determining an efficient cellular

uptake of the incorporated miRNAs[56]. The principal cationic lipids used to realize liposomes are 1,2-di-O-octadecenyl-3-trimethylammonium propane (chloride salt; DOTMA) 1,2-dioleoyl-3trimethylammonium-propane (chloride salt; DOTAP), dimethyldioctadecyl ammonium bromide (DDAB), 1,2-dioleyloxy-3dimethylaminopropane (DODMA).

Although cationic lipids are widely applied to lipid-based delivery systems, their *in vivo* applications are frequently limited by some drawbacks, such as cytotoxicity and instability[56], low sensitivity[59] and nonspecific uptake[60]. Much of these several negative consequences is directly linked to the positive charge on the surface of the particles necessary for the binding of oligonucleotides[61]. To overcome these drawbacks, neutral lipids were developed to replace the cationic lipids and serve as the non-toxic carriers for miRNA delivery[54].

Neutral lipids have the advantages that they do not form aggregates in biofluids, cannot be filtered by the liver, do not adhere to the endothelium or taken up by scavenging macrophages[55]. Neutral lipids such as cholesterol, dioleoylphosphatidyl ethanolamine (DOPE) and phosphatidylcholine (PC) can increase the stability of LNPs and decrease toxicity from cationic lipids[56].

More recently, successful tumor-inhibitory effects were reported employing a neutral lipid for the systemic delivery of synthetic miRNA mimics (miR-34a) [59].

Another possibility to reduce the negative effect of cationic lipid could be coated their coating with hydrophilic polyethylene glycol (PEG), so that minimize the interactions between the positively charged lipids and proteins that stimulate immune response, also stabilizing the complex against degradation[62].

1.4.2.1.2 Polymer-based nanoparticle delivery systems for miRNA delivery

Polymers are large molecules, or macromolecules, composed of many repeated subunits. They are characterized by different types of architecture (linear, branched and cross-linked) that affects their physical properties and various type of techniques for the synthesis (e.g. polymerization)[63].

Due to their favorable characteristics, the polymeric systems for gene delivery have attracted much attention [64]. First of all, they exhibit physicochemical properties and drug delivery rates easily tunable and controllable[26]. Moreover, could be improve the therapeutic value, the solubility and the bioavailability of the encapsulated active principles[7]. Finally, the solid nature of polymeric nanoparticles confers great stability and huge mechanical properties *in vivo*[65]. However, the cellular uptake and

degradation properties of the nanoparticles are inferior to the delivery efficiency of liposomes [26].

One of the most widely used groups of polymers for the delivery of nucleic acids to cells are cationic polymers, because, being positively charged, these can be conjugated to the negatively charged nucleic acids. In addition, they are also non-toxic, derived from renewable resources, biocompatible, biodegradable and present low immunogenicity[66] in comparison to other polymer-based systems for gene delivery.

In general, the polymers could be divided in: Synthetic polymers and Natural polymers. These two categories and the principal polymers of each group used for the nanoparticle preparation in regenerative medicine. Will be described in the rest paragraph.

1.4.2.1.2.1 Synthetic polymers

Synthetic materials, due to their many advantages, are used as effective carriers for oligonucleotides[67]. Indeed, they present a great control of their molecular composition, easy manufacturing, modification and analysis, tolerance for cargo sizes and lower immunogenicity related to viral-based vector. Moreover, compared to natural polymers, they have the advantage of sustaining the release of the encapsulated therapeutic agent over a period of days to several weeks, but they are in general limited by the use of organic solvents and relatively harsher formulation conditions[7].

However, synthetic systems are characterized by lower efficiency compared to viral vectors. Therefore, the particle size and surface properties could be modified to improve their efficiency in order to achieve specific biodistribution *in vivo*[61].

Polyethylenimine (PEI)

Polyethylenimine (PEI, Figure 12) is a class of cationic synthetic polymers with linear or branched structure, which is rich in amine groups, able to interact electrostatically

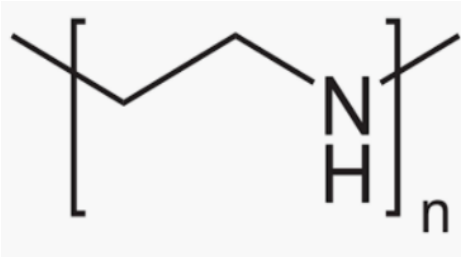

Figure 8. *Polyethyleneimine formula*

with the negative charges of the nucleic acids[56]. PEI is one of the most widely used and studied polycations for gene delivery[60].

The main advantage of the PEI-based delivery system is the rapid uptake and release (`proton sponge effect') of the nucleic acid inside the cytoplasm via an endocytic mechanism.

However, there are some limitations associated with the PEI delivery system such as poorer biodegradability inside the cell, leading to its accumulation and cytotoxicity [59] that prevent its clinical application.

A promising modification to reduce the cytotoxicity and enhance the transfection efficiency or targeted delivery of a PEI nanocarrier, is to crosslink low molecular weight PEI through a disulfide linkage[60]. Many chemical and structure modified PEIs have been explored such as polyurethane-short branch polyethylenimine (PU-PEI), the poly(L-lysine)-modified polyethylenimine (PEI–PLL) copolymer, poly(1,8-octanediocitric acid)-co-polyethylene glycol grafted with polyethyleneimine (POCG-PEI) and polylactic-co-glycolic acid (PLGA)/cetylated PEI/hyaluronic acid nanoparticles (PCPH NPs)[56].

Poly(lactide-co-glycolide) (PLGA)

Poly(lactide-co-glycolide) (PLGA) is a biodegradable, biocompatible and FDA-approved co-polyester that has been widely used for drug delivery[60]. PLGA can be hydrolyzed and broken down into nontoxic lactic acid and glycolic acid monomers and subsequently be metabolized by the body without any side effects[56]. For its ability to sustain therapeutic drug levels for prolonged periods of time[68] and its capability to encapsulate and protect nucleic acids (i.e. miRNA) from degradation, it is chosen for making nanoparticles with high production efficiency and stable mechanical property[54]. However, one of the only few drawbacks associated to PLGA-based drug delivery system is its very low targeting effects, either the passive or active ones, linked to the barren PLGA polymeric surfaces. In fact, the ester groups that compose repeating units of the whole PLGA polymer have an activity which is very low and hard to react with other functional groups[69]. Moreover, the PLGA-based nanoparticles showed low encapsulation efficiency (<50%) for low molecular weight and hydrophilic molecules[70].

According to many researches, the surface modification of PLGA nanoparticles, such as pegylation, ligand decoration or functionalization with free carboxyl (COOH) termini, were widely adopted to improve the encapsulation efficiency and pharmacodynamic control.

PEGylation can reduce the uptake of PLGA nanoparticles by the Reticulo-endotheliual system (RES)[71] and improve the NPs' circulation time in vivo and tumor uptake through the enhanced permeability and retention (EPR) effect[56]. Another modification present in literature is the incorporation of PEI in the PLGA matrix. For example, Arora et al. demonstrate a high miRNA-150 loading efficiency (78.3%) thanks this PLGA matrix variation[70]. Indeed, cationic PEI with a high positive charge density can help in encapsulation of negatively charged.

Polylactic acid (PLA)

Polylactide or polylactic acid (PLA, Figure 13) is a synthetic, thermoplastic aliphatic polyester produced from the monomer lactic acid. PLA is biocompatible, biodegradable

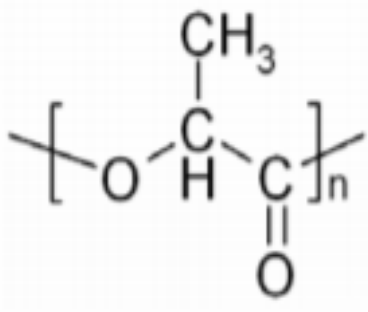

Figure 9. *Polylactic-acid formula*

and non-cytotoxic polymer, approved for human use by the US Food and Drug Administration (FDA)[68]. PLA exists in two optical forms, L-lactic acid (PLLA) and D-lactic acid (PDLA) and they form a highly regular stereocomplex with increased crystallinity. Instead the polymerization of racemic (D,L)-lactide (PDLLA) results in the formation of amorphous polymers due to the random distribution of L- and D-lactide units [72]. The two first PLA forms have slower degradation times (~2 ears) than the last PLA form (<6 months). Thanks to several benefits, such as sustainable therapeutic drug release over prolonged periods and the control of drug release kinetics, PLA is used to realized polymeric nanoparticles[73]. Moreover, using PLA to make nanoparticles the physical properties, such as size and shape, and chemical properties, including molecular weight and L:G ratio, can be easily controlled to obtain desirable pharmacokinetic and biodegradable properties[74]. PLA nanoparticles could be

prepared by solvent evaporation, solvent displacement, salting out or solvent diffusion[65].

Poly-ε-caprolactone (PCL)

PCL (poly- ε -caprolactone, Figure 14) is a hydrophobic semi-crystalline polymer, usually prepared from the ring-opening polymerization of ε -caprolactone [63].

It is highly processible, as it is soluble in a wide range of organic solvents, and able to form miscible blends with wide range of polymers [72]. PCL has a melting point ranging

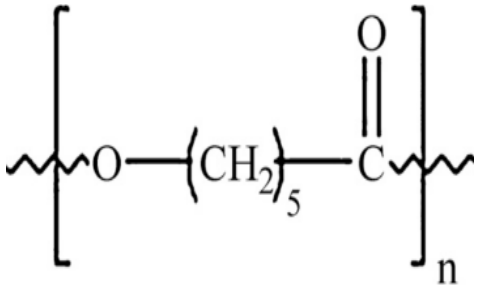

Figure 10. *Poly-ε-caprolactone formula*

from 57 and 64°C and glass transition temperature of -60°C[75]. It is characterized by a slow hydrolytic degradation (2–3 years) of its aliphatic ester linkages in physiological conditions (such as in the human body)[65].

Due to the slow degradation, high permeability to many drugs and excellent biocompatibility, PCL was initially investigated as a long-term drug/vaccine delivery vehicle and as scaffolds for tissue engineering [72]

The good solubility of PCL, its low melting point and exceptional blend compatibility has stimulated extensive research into its potential application in the biomedical field.

PCL nanoparticles could be prepared with nanoprecipitation, solvent displacement or solvent evaporation techniques[65].

1.4.2.1.2.2 Natural polymers

Natural polymeric NPs proved to be effective in stabilizing and protecting biologically active components, including vaccines, DNA, proteins, etc., from various environmental hazards and degradation. It was proved that natural polymer–based NPs

have enhanced therapeutic efficacy as a result of prolonged systemic circulation, cellular uptake, and targeted drug delivery.

Chitosan (CS)

Chitosan (CS, Figure 15) is one of the most exploited natural polymeric gene carriers[60]. It is a linear, biodegradable, biocompatible, nontoxic, mucoadhesive polymer and cationic polysaccharides[76] consisting of repeating D-glucosamine and N-acetyl-D-glucosamine units, linked via (1–4) glycosidic bonds[56]. Thanks to adjustable cationic charge density, Chitosan present a great ability to bind effectively and compact the nucleic acids[55] forming polyelectrolyte complexes with negatively charged nucleotides. Furthermore, chitosan was often used to modify PLGA nanoparticle surface

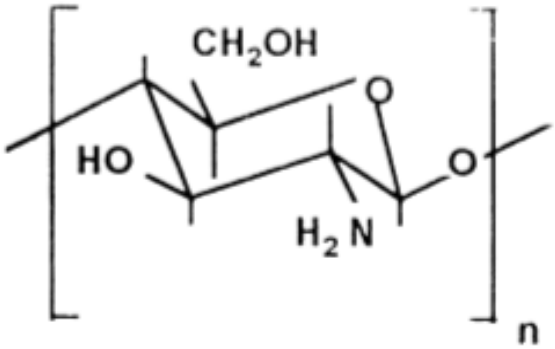

Figure 11. *Chitosan formula*

using physical adsorption and chemical binding methods in order to modify the charge of PLGA surface and improve its low targeting effects (caused by the barren PLGA polymeric surfaces)[69]. Despite the above advantages, the low transfection and delivery efficacy represent an important limit for chitosan applications[56]. This problem could be overcome optimizing the chitosan structure with modifications like thiolation, aminoethylation, cholesterol conjugation, ligand targeting, cell-penetrating peptide conjugation (CPP)[55] and acylation[77]. For example, Santos-Carballal et al. prepared the complexes

by using a degree of acetylation of chitosan (DA) of 12%. The prepared complexes had a mean diameter of less than 190nm, which is suitable for uptake by endocytosis[78].

Alginate

Sodium alginate is a water-soluble polymer that gels in the presence of multivalent cations such as calcium. Alginate particles are usually produced by dropwise extrusion of sodium alginate solution into calcium chloride solution. This method does not require specialized equipment and can be performed at ambient temperature, although the nanoparticle washing step doesn't eliminate totally the residual oil droplets. Alginate particle size depends on the size of the initial extruded droplet. The smallest particles are obtained through air atomization. The preparation of alginate nanoparticles was first achieved in a diluted aqueous sodium alginate solution in which gelation was induced by the addition of a low concentration of calcium. This leads to the formation of invisible clusters of calcium alginate gels. Alginate NPs demonstrated to be good delivery vehicles for vaccine adjuvants, such that they stabilize and protect anti-gens from the immediate biological environment, slow down antigen clearance, and enhance delivery to antigen presenting cells, especially dendritic cells.

Agarose

Agar is extracted from red algae. It is a complex mixture of polysaccharides composed of two major fractions - agarose, a neutral polymer, and agaropectin, a charged, sulfated polymer. Agarose is thermosensitive, soluble in water at high temperature > 90°C and becomes a gel at lower temperature than 50°C. Agarose nanoparticles were developed for the administration of therapeutic proteins and peptides. Agarose aqueous solution forms thermally reversible hydrogels while being cooled below the gelling temperature (318–368C). Thermal gelation results from the formation of helicoidal structures responsible for a three-dimensional network in which large amounts of water can be entrapped. The hydrogel, being hydrophilic, inert, and biocompatible, forms a suitable matrix for proteins and peptides that can be entrapped in the gel during formation. Agarose nanoparticles were produced using an emulsion-based technology that requires the preparation of an agarose solution in corn oil emulsion at 408C. Peptides and proteins to be encapsulated are initially added to the agarose solution. The small size of the dispersed aqueous nanodroplets is achieved by homogenization[79].

Chapter 2 - Materials & Methods

2.1 Materials

The two commercial synthetic polymers used in this study i.e. Poly (D,L-lactide-co-glycolide) (PLGA) 75:25 (M_W = 66000-107000 g/mol) and Poly (D,L-lactide-co-glycolide) acid terminated (PLGA-COOH) 75:25 (M_W = 4000-15000 g/mol) were purchased from Sigma Aldrich-USA and Sigma Aldrich-Germany respectively. Poly(D-glucosamine) (Chitosan) 95/100 (low molecular weight, < 10.000 Da), provided by Sigma Aldrich-USA, was used as polycation for the formation of complexes with miRNA. Poloxamer 188 (Pluronic® PE 6800 or Pluronic® F68), purchased from BASF (Aktiengesellschaft, Ludwigshafen, Germany) was used as surfactant. - NegmiR or miR-1 (miRVana™ miRNA Mimic) were purchased from Life Technologies. Milli-Q and deionized water were produced by a Millipore water purification system (Millipore Corporation). All other reagents were of analytical grade.

2.2 Methods

2.2.1 Optimization of the method for the preparation of chitosan/PLGA nanoparticles

The Nanoparticles (NPs) of Chitosan (CS) and Poly (D,L-lactide-co-glycolide)(PLGA) were prepared with nanoprecipitation technique. The CS solution (60µg/mL) was obtained by dissolving the polymer in aqueous solution of acetic acid (0,5% w/w) containing Poloxamer F68 (50% w/w related to CS). 10µL of miRNA (100 µM) were

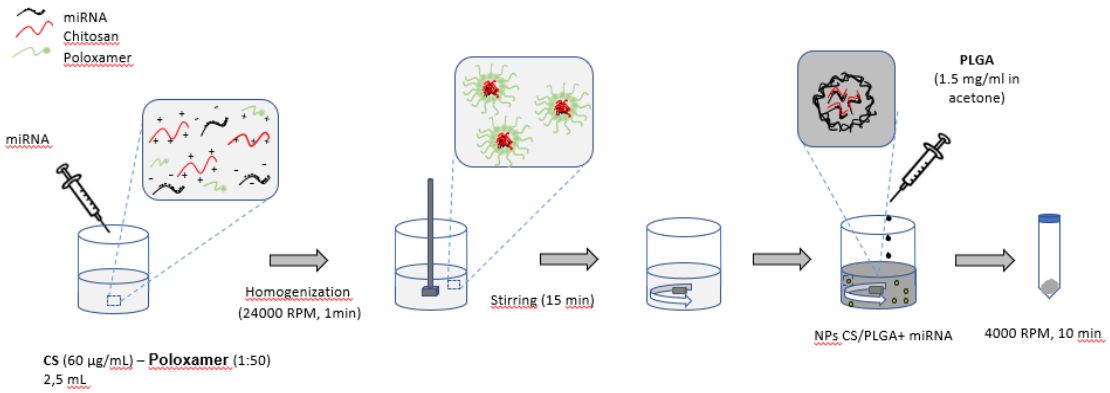

Figure 12 *Protocol for the preparation of Chitosan/PLGA nanoparticles*

added into 2.5 mL of CS/poloxamer solution. The solution was then homogenized at 24000 rpm for 1 minute and left under stirring for 15 minutes to stabilize the Chitosan/miRNA complexes. Then, 1mL of PLGA solution (1,5mg/mL) in acetone was added dropwise to the CS/miRNA-poloxamer solution to obtain PLGA-coated CS NPs. NPs were washed through centrifugation (Allegra® X-30 Series Benchtop Centrifuges, Beckman Coulter Life Sciences, USA) at 4000 rpm for 10-12 min 3 times, using centrifugal filter units (Amicon® Centrifugal Filter Units, 10 KDa cutoff), in order to wash out the residual surfactant. A schematic representation of the protocol is illustrated in **Figure 16**.

We also investigated an alternative procedure for NPs preparation with the aim to overcome toxicity and polydispersity issues observed with the previously described procedure. The modified version of the protocol is detailed in **Figure 17**. Briefly, the pH of the CS solution was maintained in a slightly acidic level of ~ 5.4 pH, by dissolving

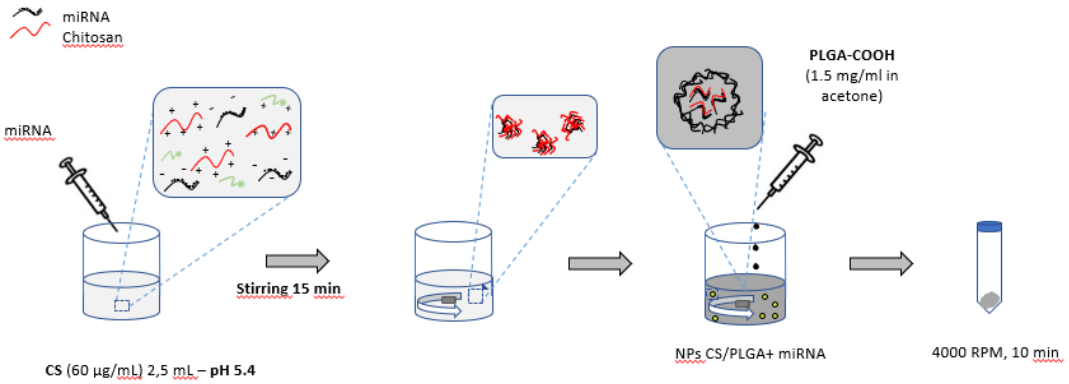

Figure 13 *Modification of the first Protocol*

CS with the minimal amount of acetic acid . We also opted for a surfactant-free design, where Poloxamer was removed and replaced with PLGA-COOH, a more hydrophilic polymer, which is expected to avoid particles coalescence and precipitation in water. The homogenization phase was removed to avoid damages to miRNA.

2.3 Physicochemical characterization of nanoparticles

2.3.1 Hydrodynamic size by dynamic light scattering (DLS)

Dynamic Light Scattering (DLS, Litesizer™ 500, Anton Paar, USA, **Figure 18**) was used to measure particle dimensions (size and polydispersity index, PDI). It is a non-invasive, well-established technique for the characterization of particles, emulsions or

Figure 14 *DLS, Litesizer™ 500, Anton Paar, USA*

molecules, which have been dispersed or dissolved in a liquid. The diameter that is measured in DLS is a value that refers to how a particle diffuses within a fluid, so it is

referred to as a hydrodynamic diameter, or rather the diameter of a sphere that has the same translational diffusion coefficient as the particle. The hydrodynamic diameter will depend not only on the size of the particle core, but also on any surface structure, as well as the concentration and type of ions in the medium. For non-spherical particles, DLS coefficient gives the diameter of a sphere that has the same translational diffusion speed as the particle.

The PDI (Polydispersity Index) is s used to estimate the average uniformity of a particle solution giving a value between 0 and 1, a low value means a tight distribution while a high value means a wide distribution due to the presence of more populations.

2.3.2 Zeta Potential analysis

Zeta potential (ζ) is the charge that develops at the interface between a solid surface and its liquid medium. In electrophoretic light scattering (ELS) the speed of the particles is measured in the presence of an electric field. The faster the particles move, the higher the zeta potential of the particles. In general, a greater magnitude zeta potential means stringer repulsion between NPs, resulting in a more stable suspension. Litesizer™ 500 uses, a novel patented (European Patent 2 735 870) technology that leads to shorter measuring times and lower applied electric fields. This means that sensitive samples can be measured with less deterioration.

2.3.3 Morphological characterization SEM (Scanning electron microscopy)

The morphological characterization of the nanoparticles was performed using a scanning electron microscope (SEM) (**Figure 15**). Before analysis, samples were placed on aluminum stabs and sputter-coated with gold, using an Agar Auto Sputter Coater. The following parameters were set: execution time of 50 s with a 30 mA deposition current.The coated samples were then imaged with a LEO 435VP SEM. Samples were analyzed with 1000x, 2000x and 5000x magnification at a working distance of 15 mm and a voltage of 20 kV.

Figure 15 *Agar Auto Sputter Coater (left) and LEO 435VP SEM (right)*

2.3.4 Fourier Transformed Infrared Spectroscopy (ATR-FTIR)

Fourier transform infrared (FTIR) spectroscopy with attenuated total reflectance (ATR) is a spectroscopy technique applied to evaluate the chemical bonds in the analyzed sample using an incident Infrared radiation (IR). In this study, ATR-FTIR Frontier FT-IR Perkin Elmer (**Figure 20**) instrument was used to investigate the surface composition of lyophilized NPs. Samples, lyophilized with a CoolSafe 4-15L freeze-dryers, (Labogene) were analyzed with a diamond crystal over a spectral range of 4000 and 600 cm^{-1}, resolution 4 cm^{-1} and 32 scans.

Figure 16 *ATR-FTIR Frontier FT-IR Perkin Elmer*

2.3.5 Evaluation of miRNA entrapment efficiency: Qubit fluorometer

Entrapment efficiency of miRNA in NPs was studied using an Invitrogen Qubit 4 Fluorometer (Thermo Fisher Scientific, US, **Figure 21**) and its dedicated analysis kit (Qubit microRNA buffer, Thermo Fisher), used according to manufacturer's protocol.

Briefly, 20 µL of the supernatant from NPs solution were mixed with 180 µL of the buffer reagent, allowed to react for 5 min, and analyzed. Qubit returns miRNA concentration (ng/mL) in the supernatant (i.e. the non-encapsultaed miRNA). The miRNA entrapment efficiency was calculated using the following formula:

$$EE(\%) = \frac{(\mu g \text{ miRNA provided} - \mu g \text{ miRNA read})}{(\mu g \text{ miRNA provided})} * 100$$

Figure 17 *Qubit 4 Fluorometer (Thermo Fisher Scientific, US)*

2.3.6 Cell viability

Cell viability was measure using Resazurin assay which produces a coloration depending on the oxidation state of the medium. The solution turns blue in an oxidized environment, while it becomes pink or colorless in a reducing environment. This assay allows monitoring of the metabolic capacity of cells, which is related to cell viability. Viable cells preserve the capacity to reduce resazurin causing fluorescence emission. Briefly, Resazurin powder was dissolved in MilliQ water (1 mg/mL), to obtain Resazurin 10X. The solution was filtered with a 0.22 um filter to avoid any bacterial contamination. Fibroblasts 3T3, were seeded in 96-well plates at a density of 2000 cells/well. After 24h, cells were treated with increasing concentrations of NPs (0.5, 1, 1.5 mg/mL) e incubated for 24 h and 48 h. After these time points, cells were washed and treated with 1 mL of medium, containing 1Xs Resazurin. The samples were incubated for 1 h to allow reaction with Resazurin. Cells were then analyzed using a plate reader (VICTOR X3, Perkin Elmer), with excitation/emission wavelength of 530/590 nm.

2.3.7 miRNA release

The miRNA release from nanoparticles has been investigated for 14 days.

Samples were incubated at 37°C to reproduce the physiological temperature. Each time nanoparticle solutions were centrifuged at 15000 rpm in order to create a pellet and 500 μL of supernatant was withdrawn and analyzed with Qubit to study the miRNA released. After that, 500 μL of Milli-Q water has been added.

2.3.8 Stability test

The complexes and nanoparticles stability have been studied for 9 days in terms of size and zeta potential in water and DMEM (with and without FBS). Samples were incubated at 37°C to reproduce the physiological temperature.

Chapter 3 - Results & Discussion

In this thesis work, NPs based on PLGA and chitosan for miRNA release were prepared and characterized by properly modifying a state-of-the art protocol [2].
The literature protocol was reproduced and in the following paragraphs its characterization results are discussed ("First method"). Then, NPs prepared by a newly developed method were characterized and the advantages of the new methods discussed ("Second method").

3.1 Preparation & characterization of miRNA-Nanoparticles (First method)

Briefly, the first method involved the preparation of a chitosan-poloxamer solution to which miRNA was added. The CS/miRNA complexes formed by homogenization and subsequent stirring phase. After that, PLGA was dropped into this mixture, in order to form bioartificial NPs based on PLGA/CS/miRNA. Finally, by a centrifugation phase, the surfactant and solvents were removed. This protocol was reproduced from literature [2].

3.1.1 Hydrodynamic size & Yield - first method

Recently miRNA-based therapies have been studied as potential alternative approaches to the current strategies used in the clinics for infarct treatment [6]. Particularly, nanoparticles have been studied as innovative tools to release miRNA to specific tissues [80].
Initially, in this thesis work, the "fist method" of preparation of NPs was analyzed, derived from literature [2].
The physicochemical characterization of NPs is usually based on their morphology characterization and particle size analysis. Indeed, size might play a fundamental role for cellular uptake and retention in the target tissues, while the polydispersity index (PDI) determines the homogeneity of size distribution [77].
DLS is generally used for particle size analysis. In this work, DLS analysis revealed that NPs possessed an average hydrodynamic size of 213±60 nm and a polydispersity of ~0.2 for blank nanoparticles, whereas miRNA-loaded NPs exhibited an average hydrodynamic size of 230±57 nm and a polydispersity index of ~0.19 (**Figure 22**a). The

size values here obtained were only slightly higher than those found in literature for the same particle type [2]. However, NPs with similar size to that obtained in this work have been reported to be internalized inside the cells by endocytosis (receptor-mediated or phagocytosis) [81]. Additionally, the standard deviation in size of NPs-First Method was quite large (around 60 nm) evidencing quite a wide size range in this method.

The Yield is the ratio between the final weight amount of obtained freeze-dried NPs over the total weight amount of starting materials (polymers) employed in the protocol. The Yield (Y%) has been obtained using the following formula:

$$Y(\%) = \frac{\text{Weight NPs}}{\text{Weight materials}} * 100$$

The blank nanoparticles showed a yield of ~37% while the miRNA-loaded nanoparticles revealed a yield of ~50%, as shown in **Figure 22**b. Yield of blank NPs was lower probably due to the lack of complexes in this formulation, decreasing the amount of chitosan binding to PLGA. On the other hand, in the miRNA-NPs, the yield was higher due to the formation of CS/miRNA complexes potentially binding to PLGA and forming bioartificial NPs. Hence it is supposed that the yield difference is mainly due to the higher loss of chitosan component when preparing blank-NPs.

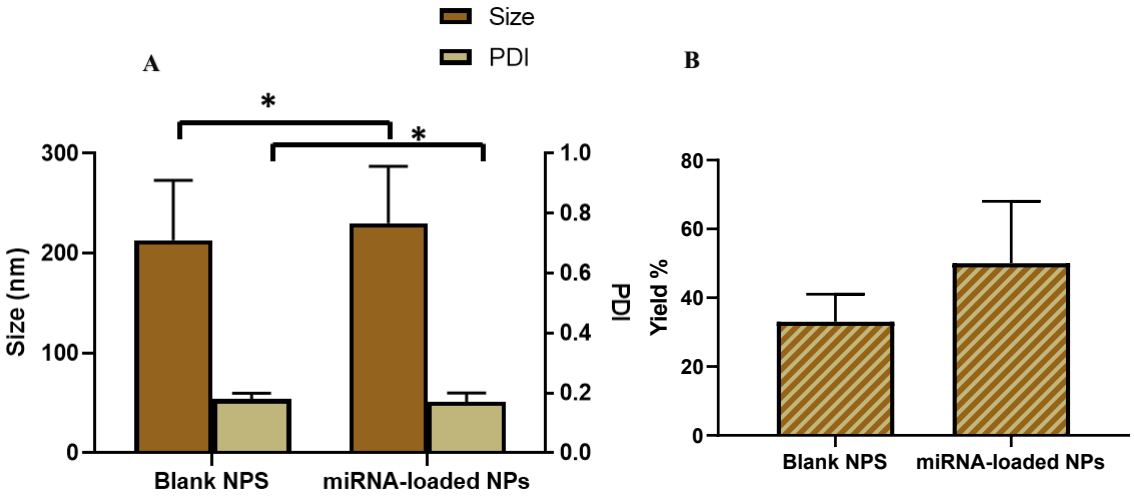

Figure 18. *Size and PDI for blank and miRNA-loaded nanoparticles* ***(A)(*p<0.05).*** *Percentage Yield* ***(b)***

3.1.2 Critical issues of the first method

The first method used for NP preparation, although derived from literature, showed a few critical issues described and faced in the following paragraphs. Such issues were revealed by physicochemical and biological characterizations of resulting NPs.

ATR-FTIR analysis was performed on NPs and their single components to analyze their chemical properties.

In **Figure 23A** the ATR-FTIR spectra for PLGA, Poloxamer and blank nanoparticles are shown.

PLGA spectrum showed characteristic bands at: 2884-3010 cm^{-1}, 1750 cm^{-1}, 1186-1089 cm^{-1} and 1450-850 cm^{-1} are due to C-H stretches, C=O stretch, C-O stretch and C-H bends.

Poloxamer spectrum showed characteristic bands at 2884 cm^{-1}, 957 cm^{-1} and 1111 cm^{-1} are due to stretching of C-H groups, C–O symmetrical structure and C–O asymmetrical stretching vibrations.

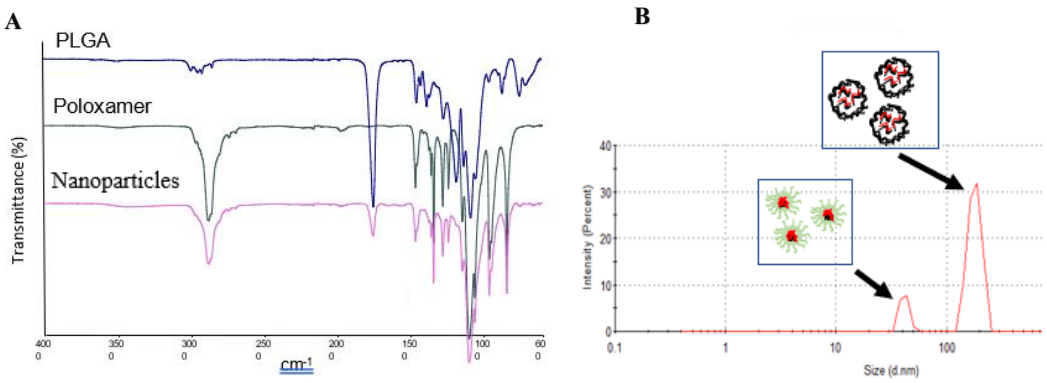

Figure 19 *ATR FTIR spectra for PLGA, Poloxamer and Blank nanoparticles* ***(a).*** *DLS pattern of miRNA-loaded nanoparticles* ***(b)***

The spectrum of NPs showed the characteristic PLGA peaks (at 1750 cm^{-1} and 1450 cm^{-1}) and also the characteristic Poloxamer peaks (at 2884 cm^{-1}, 1111 cm^{-1} and 957 cm^{-1}). ATR-FTIR analysis evidenced the presence of residual surfactant on NPs despite washing steps during their preparation. This probably resulted in the formation of Poloxamer micelles able to encapsulate CS or CS/miRNA complexes, as suggested by the DLS pattern of miRNA-NPs (**Figure 23**B) showing the presence of two NP populations. The highest pick is linked to correctly formed nanoparticles while the smallest could be linked to poloxamer micelles which were formed due to the excessive presence of the surfactant.

Another issue associated with the first method was the toxicity of prepared miRNA-loaded NPs. **Figure 24** shows that NPs with concentration of 1 mg/mL cell viability after 24h dropped to 20% and to 5% after 48h. For NP concentration of 1.5 mg/mL cell viability was 0% after 24 and 48 h. Such results were mainly attributed to the use of chitosan solution with low pH in NP preparation.

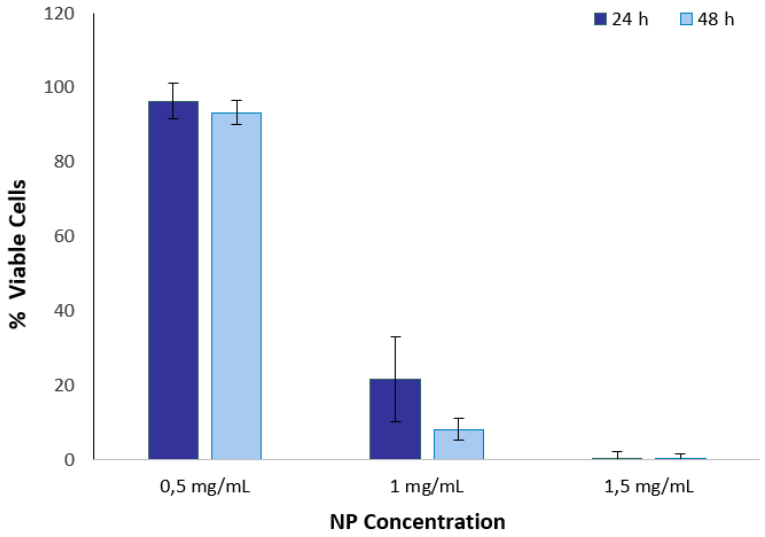

Figure 20. *Cell viability in contact with nanoparticles (first method) at different concentration*

Finally, the First method employs a homogenization phase which may be potentially detrimental for miRNA stability [82].

3.2 Optimization of the protocol for bioartificial NP preparation (second method)

In order to solve the issues associated with the first method, the protocol for the preparation of nanoparticles was modified as previously described in the section "Materials and method".

Briefly, the Poloxamer surfactant was removed and interaction between chitosan and PLGA was enhanced by employing a PLGA with terminal COOH groups (PLGA-COOH). PLGA-COOH is more hydrophilic than PLGA and allows for electrostatic interactions with chitosan.

Moreover, the homogenization phase was removed and a milder process was introduced to avoid miRNA damages.

Finally, a chitosan solution with higher pH (5.4) was employed to solve the cytocompatibility issues.

The physicochemical properties of NPs were characterized, including DLS size, Zeta Potential, Yield, Entrapment Efficiency and miRNA release.

The optimal processing parameters for NP preparations were chosen based on results.

3.2.1 Hydrodynamic size and Zeta potential – Chitosan/miRNA complexes

A preliminary study was done to analyze and optimize the CS-miRNA interaction by evaluating six different ratios between the amino groups (N) in chitosan and the phosphate groups (P) in the oligonucleotides (N/P ratio: 0.7, 1.75, 3, 5, 8, 15). By keeping the same miRNA amount, the amount of chitosan was varied consequently (CS μg: 5.5, 13.6, 23.5, 38.9, 62.3, 116.8) in order to have the different N/P ratios. This means that with increasing the N/P ratio, chitosan amount used in the formulation was progressively increased while miRNA amount was kept constant.

It is important to underline that amino groups are only partially protonated depending on the pH, hence the effective charge ratio in the formulation is lower than the theoretical one.

The aim of this study was to determine an optimal N/P ratio which allows sufficiently strong interactions for the formation of CS/miRNA complexes without hindering miRNA release.

As can be seen from the **Figure 25**A, chitosan-miRNA complex sizes increased from 170±11 nm to 450-600 nm with increasing of N/P ratio from 0.7 to 1.75-5. For N/P ratio of 1.75-5, NP size showed high variability. On the other hand, for N/P ratio of 8 and 15, the size remained constant at around 300 nm with a low variability.

Zeta Potential of complexes (**Figure 25**B) increased as a function of N/P ratio, that could be explained because of the progressively increasing amount of chitosan added to the formulations. All values were positive increasing from 3 mV for N/P ratio of 0.7 to 35 mV for N/P ratio of 15.

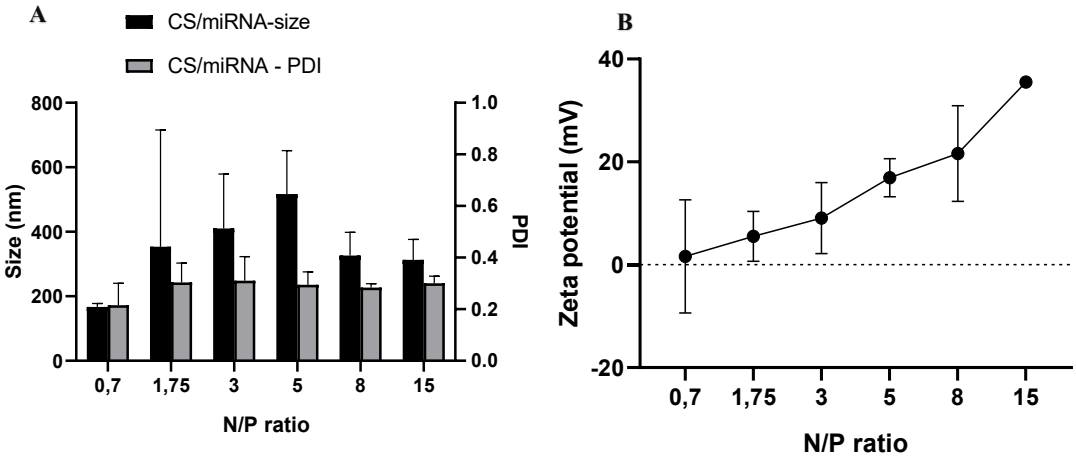

Figure 21 *Size and PDI (a) and Zeta potential (b) of CS-miRNA complexes. The miRNA amount was kept constant, while chitosan amount was progressively increased to have different N/P ratios.*

3.2.2 Hydrodynamic size and Zeta potential – Bioartificial Nanoparticles

After the formation of CS/miRNA complexes, the CS/miRNA/PLGA NPs were formed by dropping the same amount of PLGA-COOH (1.5 mg) into the solution containing CS/miRNA complexes with different N/P ratio. This means that the formed NPs all possessed the same miRNA and PLGA-COOH amount and an increased CS amount with increasing N/P ratio.

As showed in **Figure 27**A, the addition of PLGA-COOH to chitosan-miRNA complexes caused the formation of NPs with a size from 170 to 270 nm (PDI<0.25). This size range was similar to or slightly lower than chitosan complex size (**Figure 26**)

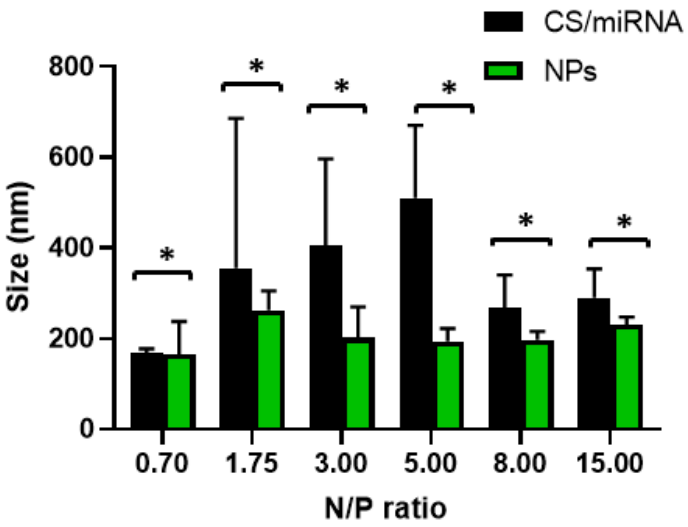

Figure 22 *Comparison between the dimensions of the complexes and their nanoparticles (*p<0.05)*

In the process a mixed population of particles probably formed including PLGA NPs, bioartificial NPs and chitosan complexes. Probably, at low chitosan amount, both PLGA and bioartificial NPs formed, while at high chitosan amount bioartificial NPs and chitosan complexes prevailed. At intermediate N/P ratio, the three populations of NPs were probably present. Surface zeta potential is a fundamental parameter to characterize the interaction of NPs with the medium. The analysis (**Figure 27**B) showed a negative value of zeta potential for bioartificial NPs with N/P ratio from 0.7 to 3 in a range of [-20, -2] mV. Zeta potential then increased with increasing N/P ratio showing positive values in a range of [5, 25] mV. This behavior was attributed to an increased chitosan amount with increasing N/P ratio. In more detail for N/P ratio from 0.7 to 3, chitosan amount was probably enough to form complexes with miRNA, which were then encapsulated within PLGA particles. When N/P ratio increased, excess chitosan coated the NP surface, with a consequent increase in zeta potential. However, particle size was not significantly affected by the change in NP composition as a function of N/P ratio, suggesting than, when excess chitosan was used, probably a mixed population of NPs was formed (including bioartificial NPs and chitosan-based complexes) or excess chitosan was lost as not incorporated into the particles. Considering that, yield analysis was performed and discussed in the next paragraph to validate the hypotheses.

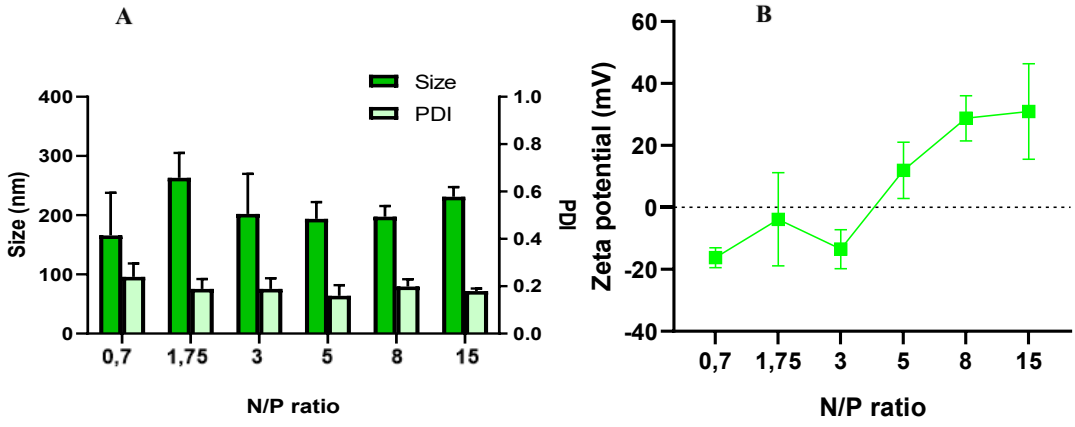

Figure 23 *Size and PDI (a) and Zeta potential (b) of miRNA-loaded bioartificial nanoparticles*

3.2.3 Yield percentage (Y%) - Nanoparticles

The yield of NP formation was evaluated, giving information on the efficiency of NP preparation.

Figure 28A illustrates Yield percentage, obtained as ratio between nanoparticles weight and the weight of materials used for the NP preparation (**Figure 28**B). The yield was around 38-40% for formulations with N/P ratio from 0.7 to 3, then it slightly increased with increasing N/P ratio, reaching 62±15% at N/P ratio of 8. However, the yield again decreased to around 40% for NPs prepared using chitosan/miRNA complexes with N/P ratio of 15.

This behavior suggested that in the case of NPs formed at N/P ratio of 0.7-3, yield remained unchanged. At N/P ratio of 5-8, probably a mixed population of NPs formed mainly consisting of bioartificial NPs and chitosan-miRNA complexes, leading to a slight increase in yield. However, at N/P ratio of 15, excess chitosan was probably unable to be encapsulated in the formulation. For this reason, the yield did not further increase for NPs prepared using N/P ratio of 15.

As compared to the First Method for NP preparation (**Figure 22**B), the yield of the Second Method of preparation was slightly lower. However, in the First Method, a substantial amount of Poloxamer surfactant was used and then remained in the NP structure, being the reason for the higher yield.

A

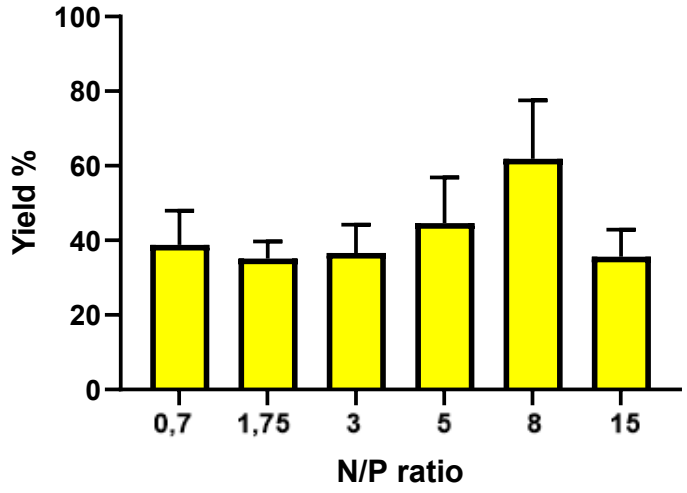

$$EY\ (\%) = \frac{Wt\ NPs}{Wt\ materials} * 100$$

B

	material (%)
0,7	
1,75	0,541
3	1,196
5	2,222
8	3,776
15	7,398

Figure 24 *Yield and respective formula (A)(**p<0.005). percentage increase in the amount of material used compared to N/ P of 0.7 (B).*

Based on previous considerations, NPs prepared from N/P ratio of 0.7 and 1.75 were not further considered for additional analyses as they probably consisted of a mixed population of blank PLGA NPs and bioartificial NPs. Similarly, particles prepared using N/P ratio of 15 were not further studied as they probably consisted of a mixed population of chitosan-miRNA complexes and bioartificial NPs.
Therefore, subsequent analyses were performed on NPs with N/P ratio of 3,5 and 8.

3.3 Characterization of shortlisted bioartificial NPs (Second method)

In this paragraph, further characterization of shortlisted bioartificial NPs and starting chitosan-miRNA complexes with N/P ratio of 3, 5 and 8 is reported including SEM analysis, Stability, Entrapment Efficiency, Release and Cell viability.

.

3.3.1 Study of stability – CS/miRNA Complexes

The chitosan-miRNA complexes stability with N/P ratio of 3, 5 and 8 in water was studied for 9 days by evaluating DLS size and zeta potential. Samples were incubated at 37°C to reproduce the physiological temperature. The aim was that to select one formulation with proper N/P ratio, allowing interactions between CS and miRNA for stable complex formation, without affecting miRNA release. As can be seen in **Figure 29**, CS/miRNA dimensions were unchanged at day 1 for all three cases. At day 2, CS/miRNA size increased for complexes with N/P ratio of 3 (728±252 nm), reaching around 1 μm at day 5-9.
On the contrary, complexes with N/P ratio of 5 were quite stable showing a size range of 250-430 nm at the tested time points.
Complexes with N/P ratio of 8 were quite stable up to day 5 (250 nm-470 nm), then they increased their size, reaching at 1.2 μm at day 7-9.

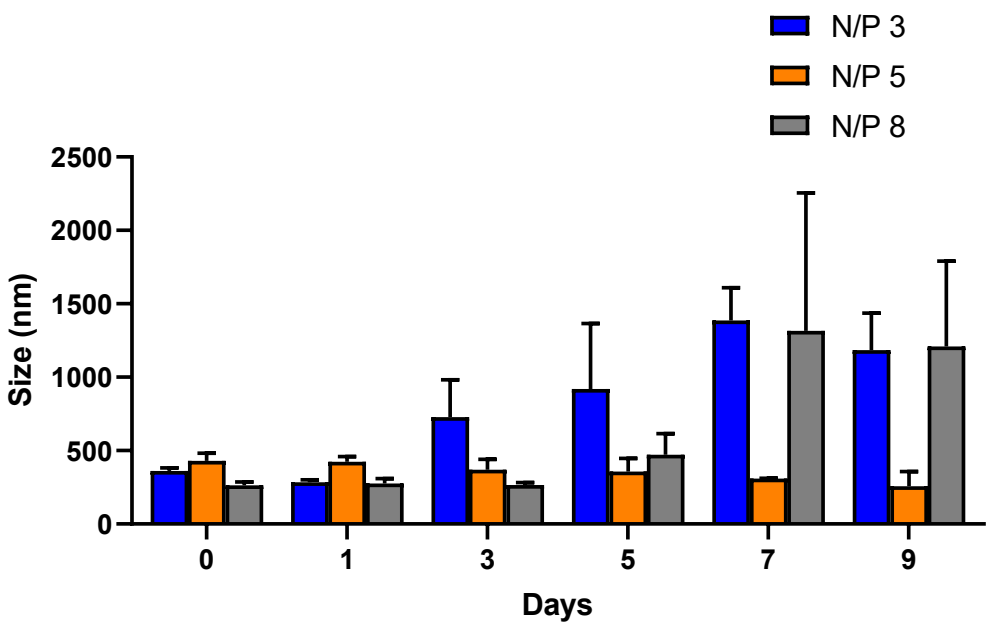

Figure 25 *Study of Chitosan-miRNA complexes stability: DLS size as a function of incubation time in water at 37°C*

.

Error! Reference source not found. reports the zeta potential of complexes as a function of incubation time.

Complexes with N/P ratio of 3 showed a stable Zeta potential for the first three days (16±6 mV), followed by a progressive decrease as a function of time. Zeta potential became negative with values of -6±4 and -10±4 mV after 7 and 9 days, respectively.

Complexes with N/P ratio of 5 showed a stable zeta potential of around 24 mV which only slightly decrease to 12±2 after 9 days.

Complexes with N/P ratio of 8 showed a stable zeta potential of about 28 mV, which progressively decreased after 5 days, reaching a value of 9±6 after 9 days.

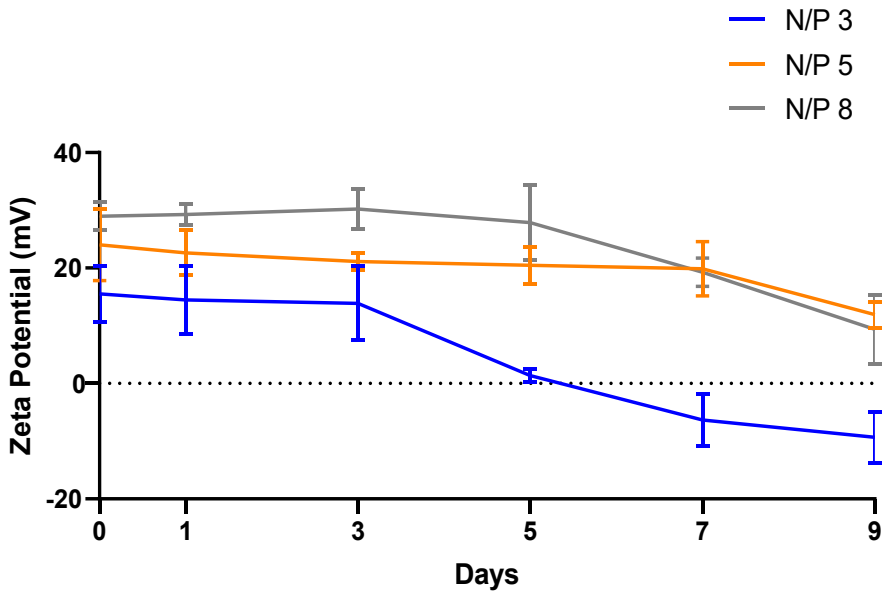

Figure 26 *Study of stability of chitosan-miRNA complexes evaluated by Zeta Potential measurements as a function of time during incubation in water at37°C.*

In conclusion, size and zeta potential analyses indicated that complexes with N/P ratio of 3 were only stable for two days, suggesting weak interactions between chitosan and miRNA. On the other hand, complexes with N/P ratio of 5 and 8 were stable for 9 days and 5 days, respectively. Based on that, complexes with N/P of 5 and 8 were further shortlisted for subsequent characterization on bioartificial NPs.

3.3.2 Study of stability – Bioartificial Nanoparticles

The long and short-term bloodstream stability is an essential requirement for a successful drug delivery to target tissues. The nanoparticles fate *in vivo* is largely determined by its capability to maintain the size, to encapsulate the drug and properly release into the cells. Ideally, the nanoparticles should remain stable until they reach the target sites. Instability of NPs causes distorted biodistribution and premature drug release, compromising the efficacy of the delivery system. Therefore, evaluation of stability is an essential aspect in nanoparticle characterization and an important factor for the success of the system.

Significant variations from the average nanoparticle size range can be interpreted as a signal of nanoparticle instability or dissociation in that specific environment or concentration.

Stability of bioartificial nanoparticle (with N/P ratio of 5 and 8) (**Figure 31**) was studied for 14 days, in terms of size and zeta potential. The samples were incubated at 37°C in order to reproduce physiological condition.

NP size was ~200 nm and appeared stable for up to 3 days. From fifth day the nanoparticles with N/P ratio of 5 (NPs_5) increased their size, reaching a size value of 1.2±0.6 μm.

NPs with N/P ratio of 8 (NPs_8) were stable up to 5 days (170±28 nm), then their size increased to 1.8 μm at 7 and 14 days.

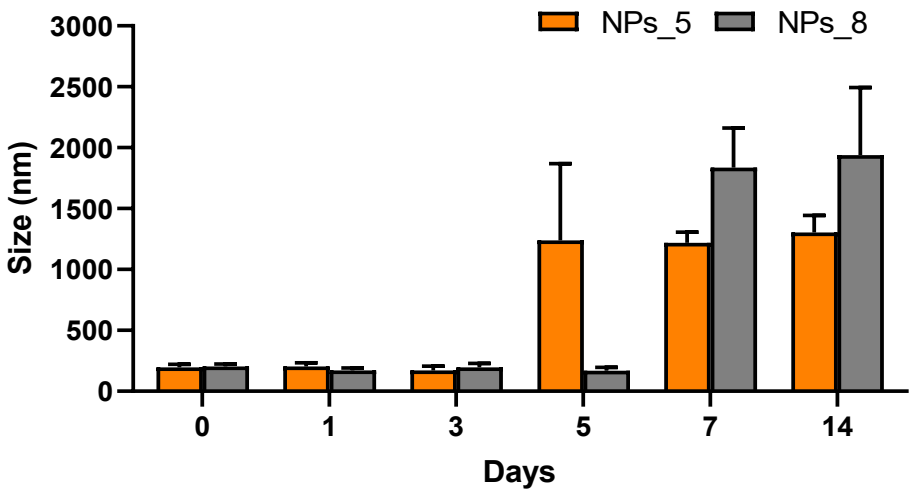

Figure 27 *Study of nanoparticles stability (Size)*

Zeta potential analysis (**Figure 32**) confirmed size results. In the case of NPs_5 zeta potential was positive (15 mV) and stable for 3 days while, after 5 days, reached a negative value of -4±1.5 mV, which was maintained up to 14 days.

NPs_8 showed a positive Zeta potential of 25-38 mV up to 5 days, then reached a negative zeta potential value of -9±4 mV and -4.5±3 mV after 7 and 14 days respectively.

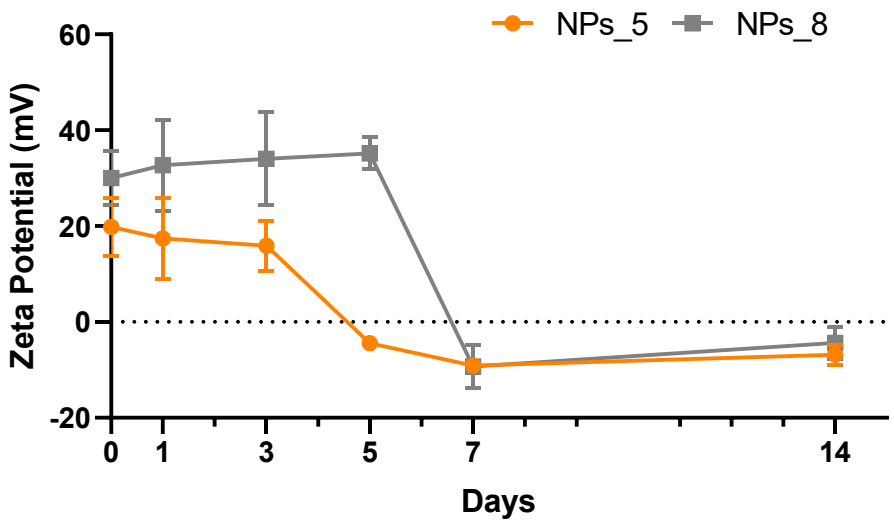

Figure 28 *Study of nanoparticles stability (Zeta potential)*

Such results suggested that bioartificial NPs were probably able to release miRNA starting from day 5 (NP_5) and day 7 (NP_8).

While chitosan-miRNA complexes with N/P ratio of 5 were more stable than those with N/P ratio of 8, their interaction of PLGA NPs changed the trend. Probably with a N/P ratio of 5 we have an amount amine groups able to create a strong interaction with phosphate groups of miRNA that does not permit a miRNA release.

3.3.3 Entrapment efficiency (EE) - Nanoparticles

The entrapment efficiency (EE) is a fundamental parameter for NPs characterization, particularly in the case of the delivery of biologically active macromolecules such as miRNA. In fact, an effective entrapment can positively influence *in vitro* cell transfection and *in vivo* therapeutic response.

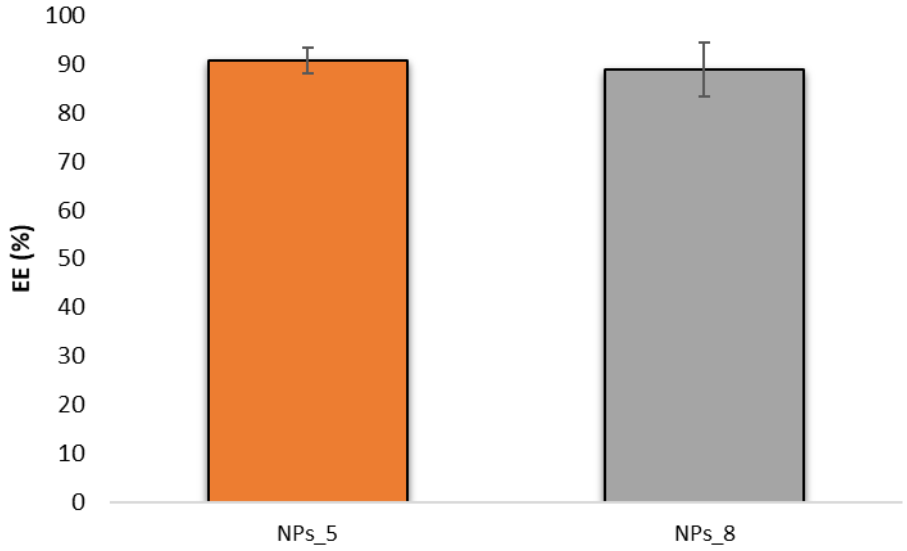

Figure 29 *Entrapment efficiency*

Error! Reference source not found. provides information about the entrapment efficiency of the bioartificial NPs with selected N/P ratio. The EE values were 90.7±3% and 89±6% for bioartificial NPs with N/P ratios of 5 and 8, respectively. Such results are in agreement with typical EE values of 78.3-95% [70][83], found in literature for drug loaded PLGA-based nanoparticles. However, they are indeed higher compared to EE of polymeric nanoparticles loaded with miRNA shown in previous studies (~85%), representing an interesting result for future application of the developed NPs [1]

3.3.4 miRNA release from bioartificial NPs

The NP release kinetics was studied by incubating NPs at 37° for 14 days.

The supernatant containing released miRNA was separated from NPs by centrifugation and miRNA was quantified by Qubit. Then, the NPs were supplemented with fresh medium, resuspended, and incubated at 37 °C. The advantage of this method is the low amount of sample requested and simple analytical equipment.

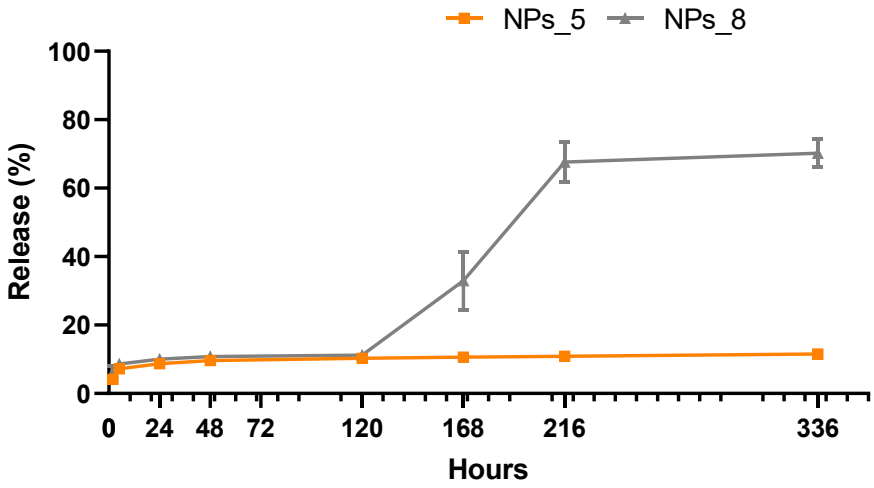

Figure 30 *miRNA cumulative release from bioartificial NPs*

Figure 34 shows that NPs with both charge ratios showed a very low release after 2 h and 5 h (< 7%) and no significant release (<10%) until fifth day. However, from 7th days the nanoparticles with N/P ratio of 8 begun to release their content, reaching 68±5% release at 9 days and releasing 70±4 % of their cargo after 14 days.

On the other hand, the NPs with N/P ratio of 5 did not release a significant amount of entrapped miRNA, reaching 11±1% release after 14 days.

These results are in agreement with the previous data obtained during the study of stability for CS/miRNA complexes and nanoparticles (**Figure 29**, **Figure 31**). In fact, although the NPs with N/P ratio of 5 showed instability at 5th day, their respective complexes were stable for 9 days (**Figure 29**, **Figure 31**). So, the interaction between chitosan and miRNA was too strong to permit a significant release. On the contrary, the nanoparticles with N/P ratio of 8 and their complexes were instable from 7th day, and indeed after 7 days they showed a significant release.

For its poor miRNA release, the NPs_5 has been rejected.

3.3.5 SEM analysis

The morphology of bioartificial NPs_8 and complexes with N/P ratio of 8 were studied by scanning electron microscopy (SEM) (**Figure 35**). This study allowed us to confirm that the nanoparticles (**Figure 35**B) have spherical shape and nanometric dimension. Moreover, the NPs_8 were able to pack respective complexes, which instead showed size distribution from nano- to micrometer (**Figure 35**A).

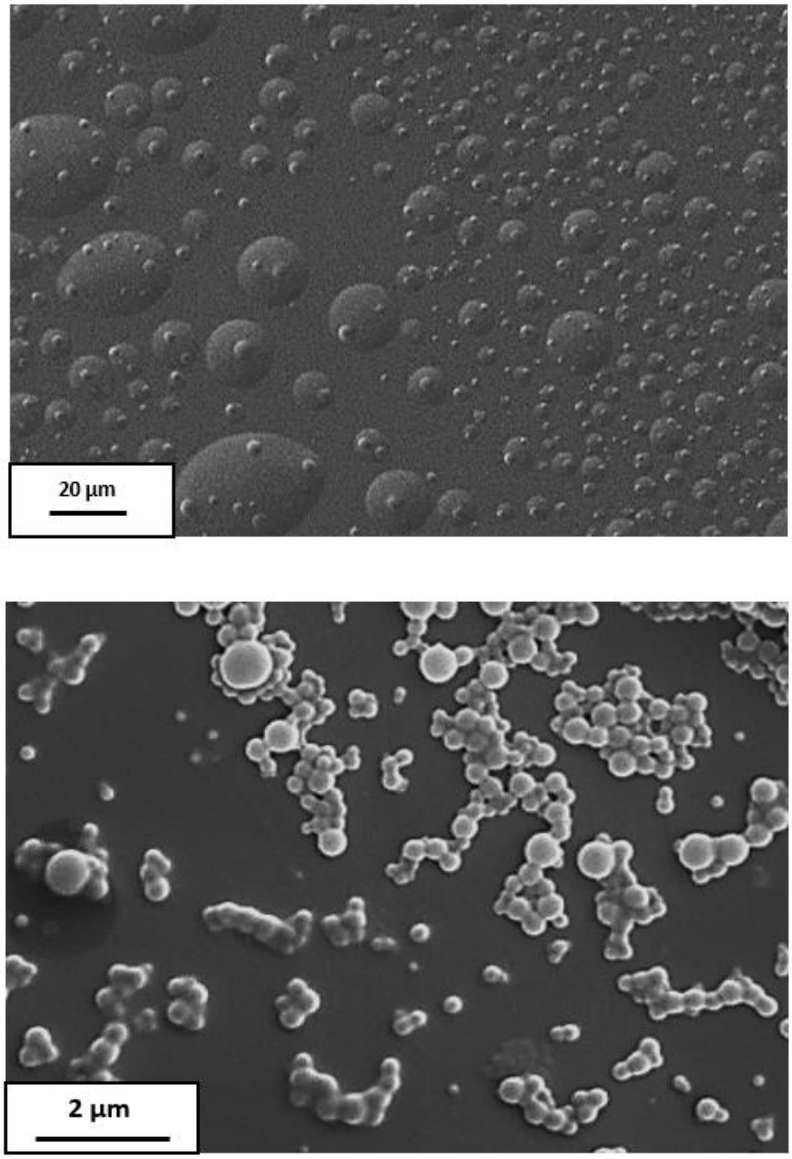

Figure 31 *Morphology analysis by SEM of CS/miRNA complexes with N/P ratio of 8 (A) and NPs_8 (B)*

3.3.6 Cell viability test: Resazurin assay

Cytotoxicity of the blank NPs_8 and miRNA-loaded NPs_8 formulated according to the second method was evaluated by resazurin assay. Fibroblasts 3T3 viability in contact with blank (**Figure 36**) and miRNA-loaded NPs (**Figure 37**) was studied in the same conditions of concentration (1.5; 1; 0.5 mg/mL) and time (24 and 48 h).

Blank NPs (**Figure 36**) showed cytocompatibility. In more detail cell viability slightly increased with NP concentration decrease: at 1.5 mg/mL concentration, viability was

around 83% and 75% after 24h and 48h respectively, while at 0.5 mg/mL concentration cell viability was around 92% after 24h and 48h, compared to control.

The viability of miRNA-loaded NPs is reported in **Figure 37**. After 24h, NPs with concentration of 0.5 and 1 mg/mL showed a cell viability of 96±4 % and 89±11% respectively. After 48h the value decrease at 78±5% for NPs with concentration of 0.5 mg/mL and 78±7 for NPs with concentration of 1 mg/mL.

A lower cell viability was observed for miRNA-NPs with 1.5 mg/mL concentration, showing a value of 70±6% after 24h and 67±2% after 48h.

Results showed the non-cytotoxicity of NPs prepared following to the second method, showing a cell viability ≥ 65-70%, that is sufficient to consider a material not cytotoxic for biomedical application [84]. However, the concentration of 1.5 mg/mL for miRNA-loaded NPs is a borderline condition with a cellular viability of 70.2±8 and 67±2 after 24h and 48h respectively. Hence, it is recommended not to use a higher amount than 1.5 mg/mL for miRNA-NPs.

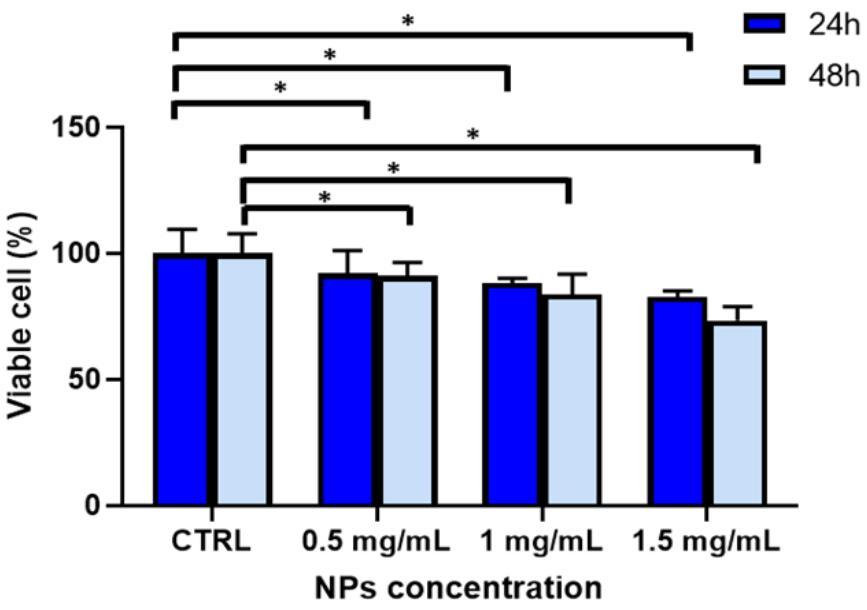

Figure 32 *Cell viability for blank nanoparticles as evaluated by resazurin assay. (*p<0.05)*

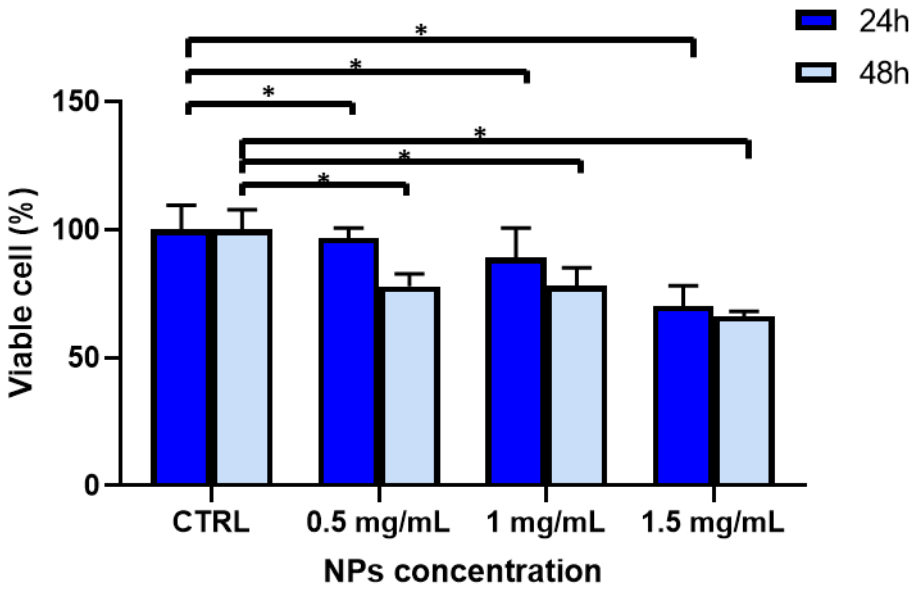

Figure 33 *Cell viability for miRNA loaded nanoparticles as evaluated by resazurin assay. (*p<0.05)*

3.3.7 Stability NPs in DMEM medium (with and without FBS)

In this study, the stability of different NPs in 10% fetal bovine serum (FBA) and 10% human plasma solution was studied by monitoring their size change. In such analysis, an increase in NP size would provide evidence of protein adsorption and, therefore, of potential instability in culture media during cell transfection and in physiologic fluids during *in vivo* application.

Figure 38 shows the size and zeta potential behavior of miRNA-loaded NPs in DMEM-FBS as a function of incubation for 7 days at 37°. Initially the size was 305±20 nm, and then increased settling at around 500 nm after 1 day. Probably, as confirmed in other studies [85], the serum protein interacted electrostatically with the nanoparticles, forming a corona around NPS that stabilized but also increased their dimensions.

A future and possible strategy to avoid protein absorption could be PEGylation [86] of NP surface that could improve systemic administration, increasing the retention time in the blood.

NP sizes in DMEM without FBS was generally higher compared to the case of DMEM-FBS during the first 3 days of incubation, then reaching similar values after 5 and 7 days incubation time.

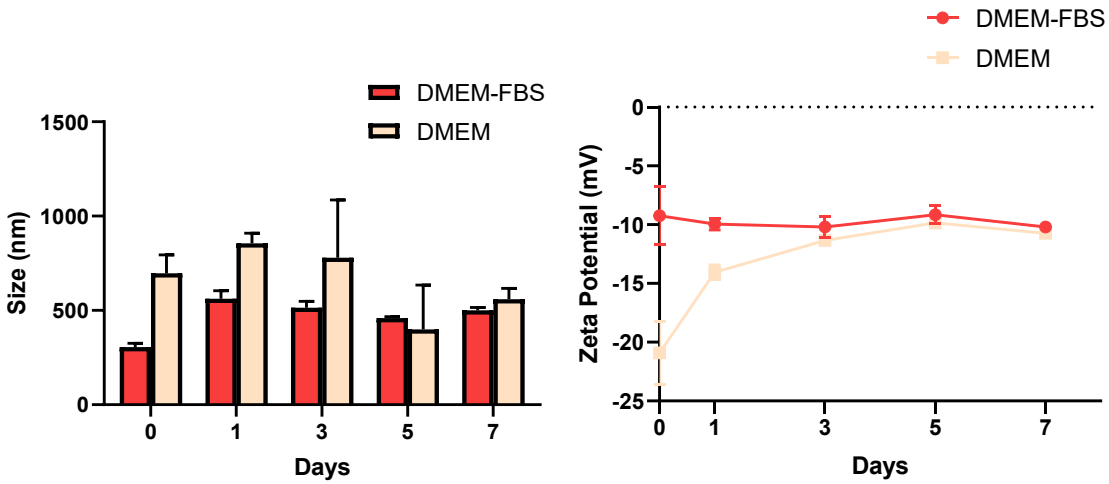

Figure 34 *Size analysis in DMEM (A) and Zeta Potential (B)*

Zeta potential of miRNA-NPs in DMEM-FBS remained constant at around -10 mV during incubation time suggesting rapid protein adsorption followed by NP stability, in agreement with size results.

On the contrary, zeta potential of NPs incubated in DMEM increased from a -20mV to -10mV after 3 days then keeping constant up to 7 days. This different behavior suggested a dynamic interaction with DMEM components during the first days, followed by stabilization, in agreement with size analysis.

Chapter 4 - Conclusion and future development

In the last years, myocardial infarction has been the leading cause of death in industrialized countries. To date, the only approach present in the clinics for heart failure treatment is the heart transplantation which, however, is associated with several drawbacks.

Based on that the scientific community is looking for new strategies that could allow myocardial regeneration, restoring the normal contractile function. Following this goal, the European project called "BIORECAR" proposes a new regenerative medicine strategy based on direct cellular reprogramming, stimulated by the injection of biomaterials capable of releasing specific factors. This project embraces the recent discovery made on specific reprogramming agents based on microRNA (or miRNA) combination [60]. In detail, Dzau's group at Duke University has shown that combinations of miRNAs (miR-Combo) can stimulate direct reprogramming of mouse fibroblasts into cardiomyocytes [3]. As an alternative to miRNA therapy using viral vectors, NPs could be used to protect oligonucleotides from degradation and to allow their efficient cell uptake and targeting ability.

The present thesis was focused on the development of bioartificial NPs for miRNA entrapment and release. The work started from the analysis of a state of the art method based on nanoprecipitation technique by elucidating its limitations (here called "First Method") [2]. PLGA was chosen as a biomaterial due to its biocompatibility, biodegradability, stable mechanical properties and because it is widely used as a polymer able to protect the drug from degradation. However, it have not a functional groups to bind with miRNA, so the PLGA only nanoparticle showed low entrapment efficiency [58]. Therefore, has been used Chitosan that which besides being biocompatible, biodegradable and not toxic, it is a polycation with positive amino groups (N) able to interact electrostatically with negative phosphate groups (P) of miRNA, increasing the entrapment efficiency. Chitosan only nanoparticles has been rejected because did not guarantee great stability and miRNA protection from degradation [78].

The "First Method" of NP preparation made use of Poloxamer as surfactant to stabilize chitosan-miRNA complexes in solution and allow their interactions with PLGA. This

method allows the formation of CS/miRNA complexes with a N/P ratio of around 19. Moreover, with the addition of the PLGA have been realized blank nanoparticles of about 210 nm and PDI of 0.18 and miRNA-loaded nanoparticles of 220 nm and PDI of 0.17 (**Figure 22**A). The Yield of the process results of around 37% and 50% for blank nanoparticles and miRNA-loaded nanoparticles respectively (**Figure 22**B).

However, some problems have been shown with this first method. First of all, the surfactant presence at the end of the process, confirmed by ATR-FTIR analysis (**Figure 23**A) was seen. This could allow the formation of Poloxamer micelles, as we can see in **Figure 23**B, besides the bioartificial nanoparticles.

Moreover, the nanoparticle solution showed problem of toxicity (**Figure 24**), since for a NPs concentration of 1mg/mL or higher the cell viability is really low (<20% after 24h). Finally, miRNA risks possible damages because the homogenization phase present in the protocol.

Therefore, a new protocol ("Second Method") was developed as mentioned in *Material and Method* section (**Figure 17**). Briefly, the pH of the CS solution was maintained in a slightly acidic level of ~ 5.4 pH, by dissolving CS with the minimal amount of acetic acid. We also opted for a surfactant-free design, where Poloxamer was removed and replaced with PLGA-COOH, a more hydrophilic polymer, which is expected to avoid particles coalescence and precipitation in water. The homogenization phase was removed to avoid possible damages to miRNA.

In more detail, different ratios between amino group of CS and phosphate groups of miRNAs (N/P ratio: 0.7, 1.75, 3, 5, 8, 15) were tested so to obtain the best interaction able to create stable CS/miRNA complexes but, at the same time, able to allow miRNA release. The **Figure 25**A illustrates how the chitosan-miRNA complex sizes increased from 170±11 nm to 450-600 nm with increasing of N/P ratio from 0.7 to 1.75-5. For N/P ratio of 1.75-5, NP size revealed high variability. On the other hand, for N/P ratio of 8 and 15, the size remained constant at around 300 nm with a low variability.

Zeta Potential of complexes (**Figure 25**B) rose as a function of N/P ratio, that could be explained because of the progressively increasing amount of chitosan added to the formulations. All values were positive increasing from 3 mV for N/P ratio of 0.7 to 35 mV for N/P ratio of 15.

The N/P ratios of 0.7 and 1.75 present a poor amount of chitosan to create strong and stable interaction with miRNA and so they present a low possibility to form CS/miRNA complexes. This could be confirmed, in **Figure 25**, by huge variability in the zeta potential and size for N/P ratio of 0.7 and 1.75 respectively. Consequently, the adding of PLGA-COOH (**Figure 27**) would lead to formation of blank PLGA-COOH

nanoparticles. For these reasons, these two ratios have been rejected. In addition, the N/P ratio of 15 presents the lowest percentage as regard the yield of the process (**Figure 28**A). Probably there is an excessive amount of chitosan and a part of it is not encapsulated in bioartificial NPs and so it is lost. So, also this ratio has been rejected.

The study of complexes stability in water has been done incubating for 9 days at 37°C the complexes with N/P of 3,5 and 8. They have been evaluated in terms of Size and Zeta potential (**Figure 29**, **Figure 30**). The results showed that the dimensions were stable for one day in all three cases. At day 2, CS/miRNA size increased for complexes with N/P ratio of 3 (728±252 nm), reaching around 1 μm at day 5-9. While its Zeta potential it's stable for the first three days (16±6 mV), followed by a progressive decrease as a function of time, reaching negative values of -6±4 and -10±4 mV after 7 and 9 days, respectively.

On the contrary, complexes with N/P ratio of 5 were quite stable showing a size range of 250-430 nm at the tested time points. Also its zeta potential results stable at around 24 mV, with a slightly decrease to 12±2 after 9 days.

Complexes with N/P ratio of 8 were quite stable up to day 5 (250 nm-470 nm), then they increased their size, reaching at 1.2 μm at day 7-9. Complexes with N/P ratio of 8 showed a stable zeta potential of about 28 mV, which progressively decreased after 5 days, reaching a value of 9±6 after 9 days.

The N/P ratio of 3 is stable for only 2 days and so rejected.

Subsequently bioartificial nanoparticles have been realized for N/P ratio of 5 and 8 and they were analyzed in terms of Stability, Entrapment Efficiency and Release.

The stability was tested in water for 14 days at 37°C, as can be seen in "*Study of stability – Bioartificial Nanoparticles"* section (**Figure 31**, **Figure 32**). NP size was ~200 nm and appeared stable for up to 3 days. From fifth day the nanoparticles with N/P ratio of 5 (NPs_5) increased their size, reaching a size value of 1.2±0.6 μm. The respective zeta potential is resulted positive (around 15 mV) and stable for 3 days while, after 5 days, reached a negative value of -4±2 mV, which was maintained up to 14 days.

NPs with N/P ratio of 8 (NPs_8) were stable up to 5 days (170±28 nm), then their size increased to 1.8 μm at 7 and 14 days. NPs_8 showed a positive Zeta potential of 25-38 mV up to 5 days, then reached a negative zeta potential value of -9±4 mV and -4.5±3 mV after 7 and 14 days respectively.

Both nanoparticle system obtained were characterized by a high miRNA entrapment efficiency (about 90%), as can be seen in "*Entrapment efficiency (EE) – Nanoparticles*" section and reported in **Figure 33**.

How described in "*miRNA release from bioartificial NPs"* section, the NPs_5 allows a really poor release of around 11% after 14 days, while after a week in NPs_8 became the release phase (~68%) and after 14 days they released a cumulative percentage of 70±4 %.

Although an excellent entrapment efficiency, the NPs_5 was not a good candidate as regard the miRNA release, so it has been rejected. The best condition is so resulted NPs_8.

This work of thesis ended by analyzing NPs_8 in terms of Cell Viability, Morphology and Stability in DMEM (with and without FBS).

The nanoparticle formulation resulted not toxic as showed in "*Cell viability test: Resazurin assay*". Indeed, we obtained a cell viability higher more than 75% for blank NPs_8 with 1.5 mg/mL concentration and 65% for miRNA-loaded NPs_8 with 1.5 mg/mL concentration. At the morphological point of view, the miRNA-loaded nanoparticles result spherical and with nanometric dimension, as confirmed by SEM study. Finally, the stability analysis in DMEM-FPS has been done incubating nanoparticles at 37° for 7 days. The study showed that the nanoparticles tend to create aggregates with the medium protein. In fact, in **Figure 38** we can see that the nanoparticle dimensions are in range of about 300-560 nm and the zeta potential is always negative with values between -9 mV and -10 mV.

Additional experiments are required to complete the characterization of the nanoparticles, for example a study on nanoparticles internalization inside the cells and the transfection capability of miRNA-loaded Nanoparticles with a therapeutic agent (miRNA-1), in order to see if the amount of reprogramming agent released is enough to cause significant effects in the cells.

Once the nanoparticles characterization will be finished, it could be interesting to functionalize the NPs with peptides in order to make them specific for target cells. Moreover, it could be possible to realize a PEG coating to avoid interactions and aggregation with serum proteins and allow systemic administration, increasing the circulation times *in vivo*.

In conclusion, the developed system is particularly promising for future application for the treatment of myocardial infarct. Furthermore, the ever-increasing number of biological activities attributed to miRNA suggests that these nanovectors can be exploited for multiple biomedical and pharmaceutical applications.

References

[1] A. Geisler and H. Fechner, "MicroRNA-regulated viral vectors for gene therapy," *World J. Exp. Med.*, vol. 6, no. 2, p. 37, 2016.

[2] D. Cosco *et al.*, "Delivery of miR-34a by chitosan/PLGA nanoplexes for the anticancer treatment of multiple myeloma," *Sci. Rep.*, vol. 5, no. December, pp. 1–11, 2015.

[3] T. M. Jayawardena *et al.*, "MicroRNA induced cardiac reprogramming in vivo evidence for mature cardiac myocytes and improved cardiac function," *Circ. Res.*, vol. 116, no. 3, pp. 418–424, 2014.

[4] Y. Sun and K. T. Weber, "Infarct scar: A dynamic tissue," *Cardiovasc. Res.*, vol. 46, no. 2, pp. 250–256, 2000.

[5] M. Ieda *et al.*, "Direct reprogramming of fibroblasts into functional cardiomyocytes by defined factors," *Cell*, vol. 142, no. 3, pp. 375–386, 2010.

[6] C. P. Hodgkinson, M. H. Kang, S. Dal-Pra, M. Mirotsou, and V. J. Dzau, "MicroRNAs and Cardiac Regeneration," *Circ. Res.*, vol. 116, no. 10, pp. 1700–1711, May 2015.

[7] J. Panyam and V. Labhasetwar, "Biodegradable nanoparticles for drug and gene delivery to cells and tissue," *Adv. Drug Deliv. Rev.*, vol. 64, no. SUPPL., pp. 61–71, 2012.

[8] E. Wilkins, W. L., K. Wickramasinghe, and B. P, "European Cardiovascular Disease Statistics 2017 edition," *Eur. Hear. Netw.*, pp. 8–15; 94, 118, 127, 149, 162, 174, 2017.

[9] E. J. Benjamin *et al.*, "Heart Disease and Stroke Statistics—2018 Update: A Report From the American Heart Association," *Circulation*, vol. 137, no. 12, pp. 130–133, Mar. 2018.

[10] N. G. Frangogiannis, "The extracellular matrix in myocardial injury , repair , and remodeling Find the latest version : The extracellular matrix in myocardial injury , repair , and remodeling," *J. Cllinical Investig.*, vol. 127, no. 5, pp. 1600–1612, 2017.

[11] A. V. Shinde and N. G. Frangogiannis, "Fibroblasts in myocardial infarction: A role in inflammation and repair," *J. Mol. Cell. Cardiol.*, vol. 70, pp. 74–82, May 2014.

[12] E. Garreta, P. Prado, J. C. Izpisua Belmonte, and N. Montserrat, "Non-coding microRNAs for cardiac regeneration: Exploring novel alternatives to induce heart healing," *Non-coding RNA Res.*, vol. 2, no. 2, pp. 93–99, 2017.

[13] S. Ounzain and T. Pedrazzini, "The promise of enhancer-associated long noncoding RNAs in cardiac regeneration," *Trends Cardiovasc. Med.*, vol. 25, no. 7, pp. 592–602, 2015.

[14] S. E. Senyo, R. T. Lee, and B. Kühn, "Cardiac regeneration based on mechanisms of

cardiomyocyte proliferation and differentiation," *Stem Cell Res.*, vol. 13, no. 3, pp. 532–541, 2014.

[15] M. A. Laflamme and C. E. Murry, "Heart regeneration," *Nature*, vol. 473, no. 7347, pp. 326–335, May 2011.

[16] A. P. Beltrami *et al.*, "Evidence That Human Cardiac Myocytes Divide after Myocardial Infarction," *N. Engl. J. Med.*, vol. 344, no. 23, pp. 1750–1757, Jun. 2001.

[17] P. Anversa, J. Kajstura, M. Rota, and A. Leri, "Regenerating new heart with stem cells," *J. Clin. Invest.*, vol. 123, no. 1, pp. 62–70, Jan. 2013.

[18] P. Anversa, A. Leri, and J. Kajstura, "Cardiac Regeneration," *J. Am. Coll. Cardiol.*, vol. 47, no. 9, pp. 1769–1776, May 2006.

[19] S. Hombach-Klonisch *et al.*, "Adult stem cells and their trans-differentiation potential—perspectives and therapeutic applications," *J. Mol. Med.*, vol. 86, no. 12, pp. 1301–1314, Dec. 2008.

[20] A. J. Wagers and I. L. Weissman, "Plasticity of adult stem cells," *Cell*, vol. 116, no. 5, pp. 639–648, 2004.

[21] L. Barile, E. Messina, A. Giacomello, and E. Marbán, "Endogenous Cardiac Stem Cells," *Prog. Cardiovasc. Dis.*, vol. 50, no. 1, pp. 31–48, 2007.

[22] S. Durrani, M. Konoplyannikov, M. Ashraf, and K. H. Haider, "Skeletal myoblasts for cardiac repair," *Regen. Med.*, vol. 5, no. 6, pp. 919–932, 2010.

[23] B. Léobon, I. Garcin, P. Menasché, J. T. Vilquin, E. Audinat, and S. Charpak, "Myoblasts transplanted into rat infarcted myocardium are functionally isolated from their host," *Proc. Natl. Acad. Sci. U. S. A.*, vol. 100, no. 13, pp. 7808–7811, 2003.

[24] A. Magenta, A. Rossini, P. Fasanaro, G. Pompilio, and M. C. Capogrossi, "MicroRNAs in Cardiac Regeneration," in *MicroRNA in Regenerative Medicine*, vol. 53, no. 9, Elsevier, 2015, pp. 917–942.

[25] A. Kawamoto *et al.*, "Intramyocardial transplantation of autologous endothelial progenitor cells for therapeutic neovascularization of myocardial ischemia," *Circulation*, vol. 107, no. 3, pp. 461–468, 2003.

[26] J. A. Kamps and G. Krenning, "Micromanaging cardiac regeneration: Targeted delivery of microRNAs for cardiac repair and regeneration," *World J. Cardiol.*, vol. 8, no. 2, p. 163, 2016.

[27] N. Witman and M. Sahara, "Cardiac Progenitor Cells in Basic Biology and Regenerative Medicine," *Stem Cells Int.*, vol. 2018, no. Figure 1, 2018.

[28] A. Mauretti, S. Spaans, N. A. M. Bax, C. Sahlgren, and C. V. C. Bouten, "Cardiac Progenitor Cells and the Interplay with Their Microenvironment," *Stem Cells Int.*, vol. 2017, 2017.

[29] K. Takahashi and S. Yamanaka, "Induction of Pluripotent Stem Cells from Mouse Embryonic

and Adult Fibroblast Cultures by Defined Factors," *Cell*, vol. 126, no. 4, pp. 663–676, 2006.

[30] V. F. M. Segers and R. T. Lee, "Stem-cell therapy for cardiac disease," no. October, 2014.

[31] M. L. Steinhauser and R. T. Lee, "Regeneration of the heart.," *EMBO Mol. Med.*, vol. 3, no. 12, pp. 701–12, Dec. 2011.

[32] Y. Y. Leong, W. H. Ng, G. M. Ellison-Hughes, and J. J. Tan, "Cardiac Stem Cells for Myocardial Regeneration: They Are Not Alone," *Front. Cardiovasc. Med.*, vol. 4, no. July, pp. 1–13, 2017.

[33] T. Y. Lu *et al.*, "Repopulation of decellularized mouse heart with human induced pluripotent stem cell-derived cardiovascular progenitor cells," *Nat. Commun.*, vol. 4, pp. 1–11, 2013.

[34] J. P. Guyette *et al.*, "Bioengineering Human Myocardium on Native Extracellular Matrix," *Circ. Res.*, vol. 118, no. 1, pp. 56–72, 2016.

[35] C. F. Leite, T. R. Almeida, C. S. Lopes, and V. J. Dias da Silva, "Multipotent stem cells of the heart-do they have therapeutic promise?," *Front. Physiol.*, vol. 6, no. MAY, pp. 1–17, 2015.

[36] C. Bearzi *et al.*, "Human cardiac stem cells," *Proc. Natl. Acad. Sci.*, vol. 104, no. 35, pp. 14068–14073, Aug. 2007.

[37] K. Urbanek *et al.*, "Myocardial regeneration by activation of multipotent cardiac stem cells in ischemic heart failure," *Proc. Natl. Acad. Sci. U. S. A.*, vol. 102, no. 24, pp. 8692–8697, 2005.

[38] K. C. Michelis, M. Boehm, and J. C. Kovacic, "New vessel formation in the context of cardiomyocyte regeneration – the role and importance of an adequate perfusing vasculature," *Stem Cell Res.*, vol. 13, no. 3, pp. 666–682, Nov. 2014.

[39] R. R. Smith *et al.*, "Regenerative potential of cardiosphere-derived cells expanded from percutaneous endomyocardial biopsy specimens," *Circulation*, vol. 115, no. 7, pp. 896–908, 2007.

[40] M. Centola, K. H. Schuleri, A. C. Lardo, and J. M. Hare, "La terapia con le cellule staminali per la rigenerazione del miocardio: Meccanismi d'azione e attuali applicazioni cliniche," *G. Ital. Cardiol.*, vol. 9, no. 4, pp. 234–250, 2008.

[41] A. Leri, J. Kajstura, and P. Anversa, "Cardiac stem cells and mechanisms of myocardial regeneration," *Physiol. Rev.*, vol. 85, no. 4, pp. 1373–1416, 2005.

[42] F. Quaini *et al.*, "Chimerism of the transplanted heart," *N. Engl. J. Med.*, vol. 346, no. 1, pp. 5–15, 2002.

[43] Y. M. Zhang, C. Hartzell, M. Narlow, and S. C. Dudley, "Stem cell-derived cardiomyocytes demonstrate arrhythmic potential," *Circulation*, vol. 106, no. 10, pp. 1294–1299, 2002.

[44] K. A. Robinson *et al.*, "Extracellular matrix scaffold for cardiac repair," *Circulation*, vol. 112, no. 9 SUPPL., pp. 135–143, 2005.

[45] S. J. Yoon *et al.*, "Regeneration of ischemic heart using hyaluronic acid-based injectable hydrogel," *J. Biomed. Mater. Res. Part B Appl. Biomater.*, vol. 91B, no. 1, pp. 163–171, Oct. 2009.

[46] A. S. Hoffman, "Hydrogels for biomedical applications," *Adv. Drug Deliv. Rev.*, vol. 64, no. March, pp. 18–23, Dec. 2012.

[47] Y.-J. Nam *et al.*, "Reprogramming of human fibroblasts toward a cardiac fate," *Proc. Natl. Acad. Sci.*, vol. 110, no. 14, pp. 5588–5593, Apr. 2013.

[48] Y. Chen, Z. Yang, Z. A. Zhao, and Z. Shen, "Direct reprogramming of fibroblasts into cardiomyocytes," *Stem Cell Res. Ther.*, vol. 8, no. 1, pp. 1–8, 2017.

[49] R. Wada *et al.*, "Induction of human cardiomyocyte-like cells from fibroblasts by defined factors," *Proc. Natl. Acad. Sci. U. S. A.*, vol. 110, no. 31, pp. 12667–12672, 2013.

[50] T. M. Jayawardena *et al.*, "MicroRNA-mediated in vitro and in vivo direct reprogramming of cardiac fibroblasts to cardiomyocytes," *Circ. Res.*, vol. 110, no. 11, pp. 1465–1473, 2012.

[51] M. Ha and V. N. Kim, "Regulation of microRNA biogenesis," *Nat. Rev. Mol. Cell Biol.*, vol. 15, no. 8, pp. 509–524, 2014.

[52] J. A. Vidigal and A. Ventura, "The biological functions of miRNAs: lessons from in vivo studies," *Trends Cell Biol.*, vol. 25, no. 3, pp. 137–147, Mar. 2015.

[53] H. Kim, D. Kim, S. H. Ku, K. Kim, S. H. Kim, and I. C. Kwon, "MicroRNA-mediated non-viral direct conversion of embryonic fibroblasts to cardiomyocytes: comparison of commercial and synthetic non-viral vectors," *J. Biomater. Sci. Polym. Ed.*, vol. 28, no. 10–12, pp. 1070–1085, 2017.

[54] Y. Chen, D.-Y. Gao, and L. Huang, "In vivo delivery of miRNAs for cancer therapy: Challenges and strategies," *Adv. Drug Deliv. Rev.*, vol. 81, no. 3, pp. 128–141, Jan. 2015.

[55] M. Muthiah, I. K. Park, and C. S. Cho, "Nanoparticle-mediated delivery of therapeutic genes: Focus on miRNA therapeutics," *Expert Opin. Drug Deliv.*, vol. 10, no. 9, pp. 1259–1273, 2013.

[56] Z. Bai *et al.*, "Non-viral nanocarriers for intracellular delivery of microRNA therapeutics," *J. Mater. Chem. B*, vol. 7, no. 8, pp. 1209–1225, 2019.

[57] B. García-Pinel *et al.*, "Lipid-based nanoparticles: Application and recent advances in cancer treatment," *Nanomaterials*, vol. 9, no. 4, pp. 1–23, 2019.

[58] D. Cosco *et al.*, "Physicochemical features and transfection properties of chitosan/poloxamer 188/poly(D,L-lactide-co-glycolide) nanoplexes," *Int. J. Nanomedicine*, vol. 9, no. 1, pp. 2359–2372, 2014.

[59] A. Ganju *et al.*, "miRNA nanotherapeutics for cancer," *Drug Discov. Today*, vol. 22, no. 2, pp. 424–432, Feb. 2017.

[60] B. Peng, Y. Chen, and K. W. Leong, "MicroRNA delivery for regenerative medicine," *Adv.*

Drug Deliv. Rev., vol. 88, pp. 108–122, 2015.

[61] Y. Zhang, Z. Wang, and R. A. Gemeinhart, "Progress in microRNA delivery," *J. Control. Release*, vol. 172, no. 3, pp. 962–974, Dec. 2013.

[62] D. M. Pereira, P. M. Rodrigues, P. M. Borralho, and C. M. P. Rodrigues, "Delivering the promise of miRNA cancer therapeutics," *Drug Discov. Today*, vol. 18, no. 5–6, pp. 282–289, 2013.

[63] R. Chandra, "Biodegradable polymers," *Prog. Polym. Sci.*, vol. 23, no. 7, pp. 1273–1335, Nov. 1998.

[64] X. Niu, W. Zou, C. Liu, N. Zhang, and C. Fu, "Modified nanoprecipitation method to fabricate DNA-loaded PLGA nanoparticles modified nanoprecipitation method," *Drug Dev. Ind. Pharm.*, vol. 35, no. 11, pp. 1375–1383, 2009.

[65] A. Kumari, S. K. Yadav, and S. C. Yadav, "Biodegradable polymeric nanoparticles based drug delivery systems," *Colloids Surfaces B Biointerfaces*, vol. 75, no. 1, pp. 1–18, 2010.

[66] S. K. Samal *et al.*, "Cationic polymers and their therapeutic potential," *Chem. Soc. Rev.*, vol. 41, no. 21, pp. 7147–7194, 2012.

[67] K. A. Whitehead, R. Langer, and D. G. Anderson, "Knocking down barriers: Advances in siRNA delivery," *Nat. Rev. Drug Discov.*, vol. 8, no. 2, pp. 129–138, 2009.

[68] A. Manuscript, "Biodegradable Nanoparticles for Cytosolic," vol. 59, no. 8, pp. 718–728, 2008.

[69] Y. Wang, P. Li, and L. Kong, "Chitosan-modified PLGA nanoparticles with versatile surface for improved drug delivery," *AAPS PharmSciTech*, vol. 14, no. 2, pp. 585–592, 2013.

[70] S. Arora *et al.*, "Synthesis, characterization, and evaluation of poly (D,L-lactide-co-glycolide)-based nanoformulation of miRNA-150: Potential implications for pancreatic cancer therapy," *Int. J. Nanomedicine*, vol. 9, no. 1, pp. 2933–2942, 2014.

[71] G. Arora, J. Shukla, S. Ghosh, S. K. Maulik, A. Malhotra, and G. Bandopadhyaya, "Plga nanoparticles for peptide receptor radionuclide therapy of neuroendocrine tumors: A novel approach towards reduction of renal radiation dose," *PLoS One*, vol. 7, no. 3, pp. 1–11, 2012.

[72] L. S. Nair and C. T. Laurencin, "Biodegradable polymers as biomaterials," *Prog. Polym. Sci.*, vol. 32, no. 8–9, pp. 762–798, 2007.

[73] C. M. Luz *et al.*, "Poly-lactic acid nanoparticles (PLA-NP) promote physiological modifications in lung epithelial cells and are internalized by clathrin-coated pits and lipid rafts," *J. Nanobiotechnology*, vol. 15, no. 1, pp. 1–18, 2017.

[74] B. K. Lee, Y. Yun, and K. Park, "PLA micro- and nano-particles," *Adv. Drug Deliv. Rev.*, vol. 107, no. 3, pp. 176–191, Dec. 2016.

[75] D. K. Armani and C. Liu, "Microfabrication technology for polycaprolactone, a biodegradable polymer," *J. Micromechanics Microengineering*, vol. 10, no. 1, pp. 80–84,

2000.

[76] E. K. Efthimiadou, A.-F. Metaxa, and G. Kordas, “Modified as Drug Delivery,” in *Polysaccharides*, no. August, Cham: Springer International Publishing, 2014, pp. 1–26.

[77] X. P. Guan, D. P. Quan, K. R. Liao, W. Tao, X. Peng, and K. C. Mai, “Preparation and characterization of cationic chitosan-modified poly(D,L-lactide-co-glycolide) copolymer nanospheres as DNA carriers,” *J. Biomater. Appl.*, vol. 22, no. 4, pp. 353–371, 2008.

[78] M. Denizli *et al.*, “Chitosan Nanoparticles for miRNA Delivery,” in *Methods in molecular biology (Clifton, N.J.)*, vol. 1632, 2017, pp. 219–230.

[79] C. Pinto Reis, R. J. Neufeld, A. J. Ribeiro, and F. Veiga, “Nanoencapsulation I. Methods for preparation of drug-loaded polymeric nanoparticles,” *Nanomedicine Nanotechnology, Biol. Med.*, vol. 2, no. 1, pp. 8–21, 2006.

[80] S. W. L. Lee *et al.*, “MicroRNA delivery through nanoparticles,” *J. Control. Release*, vol. 313, no. October, pp. 80–95, 2019.

[81] S. A. Kulkarni and S. S. Feng, “Effects of particle size and surface modification on cellular uptake and biodistribution of polymeric nanoparticles for drug delivery,” *Pharm. Res.*, vol. 30, no. 10, pp. 2512–2522, 2013.

[82] S. L. Pal, U. Jana, P. K. Manna, G. P. Mohanta, and R. Manavalan, “Nanoparticle: An overview of preparation and characterization,” *J. Appl. Pharm. Sci.*, vol. 1, no. 6, pp. 228–234, 2011.

[83] S. Shi *et al.*, “Dual drugs (microRNA-34a and paclitaxel)-loaded functional solid lipid nanoparticles for synergistic cancer cell suppression,” *J. Control. Release*, vol. 194, pp. 228–237, 2014.

[84] L. Montanaro *et al.*, “Cytotoxicity, blood compatibility and antimicrobial activity of two cyanoacrylate glues for surgical use,” *Biomaterials*, vol. 22, no. 1, pp. 59–66, 2000.

[85] H. T. R. Wiogo, M. Lim, V. Bulmus, J. Yun, and R. Amal, “Stabilization of magnetic iron oxide nanoparticles in biological media by fetal bovine serum (FBS),” *Langmuir*, vol. 27, no. 2, pp. 843–850, 2011.

[86] J. S. Suk, Q. Xu, N. Kim, J. Hanes, and L. M. Ensign, “PEGylation as a strategy for improving nanoparticle-based drug and gene delivery,” *Adv. Drug Deliv. Rev.*, vol. 99, pp. 28–51, Apr. 2016.